N 70 28549
NASA CR-72673

FINAL REPORT

DEVELOPMENT OF HIGH TEMPERATURE OXIDATION RESISTANT COATINGS FOR CHROMIUM-BASE ALLOYS

By

H. A. FISCH and J. C. SAWYER

Prepared for

NATIONAL AERONAUTICS AND SPACE ADMINISTRATION

CONTRACT NAS 3-11173

NASA Lewis Research Center
Joseph R. Stephens, Research Advisor
John P. Merutka, Project Manager
Materials and Structures Division

Request for copies of this report should be referred to

National Aeronautics and Space Administration
Office of Scientific and Technical Information
Attention: AFSS-A
Washington, D. C. 20546

NASA CR-72673

FINAL REPORT

DEVELOPMENT OF HIGH TEMPERATURE OXIDATION RESISTANT COATINGS FOR CHROMIUM-BASE ALLOYS

BY

H. A. Fisch and J. C. Sawyer

TRW INC.
23555 Euclid Avenue
Cleveland, Ohio 44117

Prepared for

NATIONAL AERONAUTICS AND SPACE ADMINISTRATION

October 13, 1969

CONTRACT NAS 3-11173

NASA Lewis Research Center
Cleveland, Ohio
Joseph R. Stephens, Research Advisor
John P. Merutka, Project Manager
Materials and Structures Division

FOREWORD

The research described in this report was conducted by TRW Inc. under NASA Contract NAS 3-11173. The work was done under the direction of the NASA Project Manager, Mr. John P. Merutka, Materials and Structures Division, NASA-Lewis Research Center. Mr. Joseph R. Stephens, Materials and Structures Division, NASA-Lewis Research Center, was the research advisor.

This report has also been issued as TRW internal report number ER-7397.

Prepared by: H. A. Fisch

H. A. Fisch

Approved by: E. A. Steigerwald

E. A. Steigerwald

ABSTRACT

An investigation was conducted to develop coating systems for protecting chromium base alloys from degradation in high temperature air environments. Three coating systems were studied on a Cr-7Mo-2Ta substrate. These were: (1) titanium modified chromium silicide (Cr-Ti-Si) formed directly on the substrate, (2) Cr-Ti-Si formed on an intermediate Cr-MgO barrier layer and, (3) Cr-Ti-Si formed on an intermediate Cr-Y-MgO barrier layer.

Based on weight gain after 200 hours of cyclic oxidation testing in air at 2100°F (1422°K), titanium modified chromium silicide coating formed directly on the alloy was the most protective and the Cr-Y-MgO/Cr-Ti-Si the least protective.

After 100 and 200 hours exposure, the nitrogen content of the substrate was raised from 0.0022 weight percent to typically 0.008 and 0.010 weight percent respectively. Although nitrogen contamination could be a contributing factor, the increase in bend transition temperature of the substrate from about 540°F (560°K) to above 1490°F (1083°K) was attributed to an effect of thermal treatment during coating processing.

TABLE OF CONTENTS

TABLE OF CONTENTS (Continued)

LIST OF TABLES

LIST OF FIGURES

LIST OF FIGURES (Continued)

SUMMARY

The objective of this program was to develop and evaluate coatings which would offer protection to chromium-base alloys from oxidation and nitrogen contamination without substantially increasing the bend transition temperature.

A process development program was performed and coatings were prepared for cyclic oxidation tests. Two of these coatings were titanium modified chromium silicide (Cr-Ti-Si) formed directly on Cr-7Mo-2Ta. Two were barrier layer coatings nominally consisting of six and twelve volume percent MgO in chromium which were titanized and silicided. The remaining two were barrier layer coatings consisting of nominally six and twelve volume percent MgO in chromium 0.3 w/o yttrium which were titanized and silicided.

Coated and uncoated Cr-7Mo-2Ta specimens were cyclic oxidation tested for 200 hours in air at 2100°F (1422°K). After exposure, all of the coatings had spalled to varying degrees with the Cr-Ti-Si (heavy) system showing the least spalling. The total nitrogen content of the substrate was essentially the same for all samples and was typically 0.008 weight percent after 100 hours exposure and 0.01 weight percent after 200 hours exposure compared to 22 ppm prior to exposure. The surface oxide on coated specimens of Cr-7Mo-2Ta after exposure was Cr_2O_3. In many cases TiO_2 was observed as well as unidentified compounds believed to be complex silicates, silicides or oxides.

Metallographic examination of the barrier layer coatings as-formed and after oxidation testing revealed a region of porosity which was thought to have resulted from an instability of the MgO particles during the coating formation process.

Electron microprobe examinations were made of the uncoated Cr-7Mo-2Ta alloy and three coating systems: Cr-Ti-Si(light), Cr-Ti-Si(heavy), and a Cr-12MgO barrier layer coating system. The as-received alloy was characterized by tantalum and yttrium segregation. In the as-formed Cr-Ti-Si(light and Cr-Ti-Si(heavy) coatings, molybdenum and tantalum were detected in the coating layer, but were not found in the barrier-layer coating.

Measurements of the bend transition temperature showed that while uncoated Cr-7Mo-2Ta was ductile at 1090°F (861°K), all of the coated specimens tested after 100 or 200 hours of cyclic oxidation exposure were brittle at 1420-1490°F (1055-1083°K). An as-coated Cr-Ti-Si(light) coupon and an uncoated coupon which were given a thermal treatment identical to that used in the coating cycle also were brittle at 1490°F (1083°K) indicating that the relatively high temperature associated with the coating method could have produced embrittlement. The overall results indicated that the coating concepts evaluated did not produce useable coatings for chromium alloys.

INTRODUCTION

The continued improvement of aircraft gas turbine engines requires higher operating temperatures for increased fuel efficiency, improved specific thrust and lower engine weights. To achieve this objective materials capable of withstanding the increasingly severe service environments that are imposed by the higher operating temperatures must be developed. Potential materials for blades in engines operating above 2000°F (1360°K) are cermets, fiber reinforced metals, refractory metal alloys and chromium-base alloys. The utility of cermets is limited by brittleness and poor fatigue resistance and fiber reinforced materials are still in the development stage. Refractory alloys, e.g., tantalum and tungsten are at a disadvantage for use as rotating hardware such as turbine blades because of their relatively high densities. Moreover, some refractory alloys have high ductile-to-brittle transition temperatures (DBTT) and all require coatings for protection against oxidation.

The relatively low density of chromium (7.19 g/cm^3), which is less than that of nickel-base and cobalt-base superalloys, high melting point, 3410°F (2150°K), freedom from allotropic transformations, adequate strength on alloying and better oxidation resistance when compared with refractory metals make it an attractive material for use in blades and vanes. The major limitation to the use of chromium alloys in air breathing gas turbine engines is their susceptibility to nitrogen embrittlement, high vapor pressure, and marginal oxidation resistance. Work toward reducing nitrogen embrittlement has followed two paths; alloying with nitride forming elements such as yttrium, lanthanum or thorium (1, 2)* and protection by nitridation and oxidation resistant claddings or coatings. Based on appearance and weight gains, gas-pressure bonded cladding of Ni-20Cr-20W foil protected Cr-5W-0.1Y for times in excess of 600 hours at 2100°F (1420°K) (3). However, the DBTT was increased to at least 1000°F (810°K) after 100 hours at 2100°F (1430°K) compared to 500°F (530°K) for unexposed specimens. Among other coating systems investigated, aluminum and iron-aluminum coatings on Cr-5W-0.1Y (4) showed the lowest weight gains after exposure to air at 2100°F (1420°K); however, the DBTT was raised to above 1600°F (1140°K). Simple silicide coatings (5) protected Cr-5W-0.1Y for times to 500 hours at 2000°F (1366°K) without oxygen or nitrogen penetration into the substrate. Boride, aluminide and silicide coatings have also been investigated on Cr-0.17Y and Cr-5W-0.18Y substrates (6). Boride coatings were unsatisfactory due to poor oxidation and nitridation resistance. The aluminide coatings were undesirable because the substrate was embrittled by inward diffusion from the coating. The unmodified silicide was not promising as a coating because the DBTT of the coated and 2100°F (1420°K) air-exposed specimens was raised to 700°F (640°K) from the original 200°F (366°K) for

the uncoated alloy. An iron modified silicide coating was found to protect Cr-0.17Y and Cr-5W-0.18Y against oxidation and nitridation for 100 hours at 2100°F (1420°K). Other more highly alloyed silicide modifiers which protected Cr-0.17Y were Fe-Mo-W, Fe-Mo-W-Ti and V-Mo-W-Ti. These results show that specific modified silicide coatings have desirable features and offer potential for protecting chromium, but further work is required to achieve oxidation resistance without an accompanying increase in the DBTT.

With this as a background, TRW Inc., with the support of NASA Lewis, undertook a program of investigation to further develop coatings for chromium. Two chromium-base alloys, Cr-5W-0.1Y and Cr-7Mo-2Ta-0.1Y were supplied by NASA for use in this program. In conceptual form, the coating systems investigated consisted of two layers. An outer oxidation resistant coating and an intermediate layer formed directly on the chromium alloy substrate. The intermediate layer was intended to act as a barrier or sink to prevent the diffusion of nitrogen into the substrate and also to reduce the vaporization of chromium.

The preparation of two coating systems, a silicide-sink system and a Kanthal (Fe-25Cr-3Co-4Al)-sink system was investigated. The silicide sink system consisted of an exterior titanium modified chromium silicide separated from the chromium alloy substrate by an intermediate sink layer of either chromium in which MgO particles were dispersed or prealloyed chromium-yttrium with dispersed MgO particles. The Kanthal-sink system consisted of an outer layer of Kanthal separated from the substrate by either of two intermediate barrier layers; an iron-MgO dispersion alloy or a prealloyed iron-yttrium layer in which MgO particles were dispersed. In all cases a titanium-modified chromium silicide coating, without any intermediate sink layer, served as a reference coating for these systems. The effectiveness of the coatings was evaluated by testing in an air environment at 2100°F (1420°K).

The objective of this program was to develop and evaluate these coatings for protecting chromium-base alloys against oxidation and nitridation at 2100°F (1420°K).

MATERIALS

The substrate alloys used in this work were supplied by NASA Lewis. Preliminary work was done using a nominal Cr-5W-0.1Y alloy (Heat 84-100) prepared under a separate NASA sponsored program (7) (NAS 3-7901 and NAS 3-7919). The material used for the major portions was a complex Cr-7Mo-2Ta-0.09C-0.1Y alloy (Heat 140-100 and 131-100) which was also prepared under a separately sponsored NASA program (8) (NAS 3-9417). The analyses for both of these substrate alloys are given in Table I. The vendor analyses of the powders used to form the intermediate coating layers are given in Table II, and the analyses of the prealloyed Cr-Ti powder, used to form the titanized layer and the silicon powder used for siliciding are given in Table III.

SAMPLE PREPARATION AND TEST PROCEDURES

The standardized procedures which were used for the initial preparation of samples and subsequent evaluation of the applied coatings are discussed in this section. Since various techniques for applying the coatings were used, each will be described in the Coating Development section of this report.

Sample Preparation

The alloys were received from NASA Lewis as 1 inch (25.4mm) by 2 inch (50.8mm) coupons. The Cr-5W-0.1Y coupons were nominally 0.027 inch (0.69mm) thick and the Cr-7Mo-2Ta-0.09C-0.1Y coupons were nominally 0.060 inch (1.52mm) thick.

In order to provide better conditions for coating application, corners and edges of the specimens were rounded by hand filing. The specimens were then electropolished using the electrolytes and operating conditions given in Table IV. Before using the bath, it was conditioned by polishing unalloyed chromium coupons until the color became dark green. After electropolishing, the test coupons were vapor blasted and rinsed in isopropanol before applying the coating layers.

Cyclic Air Exposure Testing

To evalute the oxidation resistance of the coatings, one inch (25.4mm) by two inch (50.8mm) specimens were supported on silica pads in a box furnace and exposed to slowly flowing air at 2100°F (1420°K). Uncoated coupons were placed on alumina pads. The temperature was held $\pm$ 10°F (5°K) of the control temperature. The hot zone of the furnace was 12 X 10 X 8 inches (305 X 254 X 203mm) and the air flow rate was four volume changes per hour. Each coating system was tested in triplicate, with one specimen being removed for evaluation after 100 hours exposure and the remaining samples after 200 hours exposure time had been accumulated. For the first 20 hours the specimens were cooled to room temperature, visually examined and weighed after successive 2 hour exposures at temperature. Thereafter, 20 hour cycles were used between cooling and examinations. The specimens were weighed after removal from the furnace, lightly brushed and reweighed. After each exposure period the specimens were turned over so that the surface previously resting on the pad was exposed to the furnace atmosphere. At the end of 100 or 200 hour exposures the specimens were subjected to metallographic and chemical analysis.

Metallography and Chemical Analysis

The uncoated and coated coupons were examined as-prepared and after oxidation testing to determine the microstructural characteristics

of the coating layers, i.e., the extent of interdiffusion of coating, substrate, and nitrided layer. Metallographic samples were examined as polished and after etching. The electrolyte etchant used to determine nitride precipitation in the matrix beneath the coating layers was a 10 part concentrated sulphuric acid and 90 part water solution. Microhardness profile measurements on as-coated and oxidation tested coupons were made from the outer surface of the coating into the matrix using a Knoop indenter with a 50 gram load. The extent of interdiffusion of major elements was evaluated using an electron microprobe analyzer in the beam scanning X-ray raster mode, and the composition of the surface oxidation products was investigated by X-ray diffraction.

Chemical analysis, using a micro Kjeldahl technique, was made for nitrogen contamination in the substrate. Before making the analysis the coating layer was removed by dissolution in a mixture, consisting of 1 part 60 percent hydrofluoric acid and one part water, which did not attack the Cr-7Mo-2Ta alloy. The coating was considered to have been removed when no further bubbling action was observed. The oxide on the uncoated specimens was removed by immersing them in a hot caustic solution containing 120g/l NaOH and 37.4g/l $KMnO_4$ at 200°F (366°K) for 45 minutes. This was followed by an eight minute immersion in an aqueous solution consisting of 35 volume percent concentrated HNO_3 plus 14 volume percent "Nitradd"*. The successive treatments were repeated as many times as necessary to completely remove the oxide.

Measurement of Bend Transition Temperature

The bend transition temperature was evaluated in accordance with Materials Advisory Board recommended procedures (9). The test specimens were 2 inch (50.8mm) by 1 inch (25.4mm) X 0.060 inch (1.5mm) and were tested in the longitudinal, i.e., 2 inch (50.8mm) direction. Samples were bent over a 4T mandrel using three-point loading, the end loading points being one inch (25.4mm) apart. The bend equipment was contained in an electrically heated furnace.

---

* Proprietary trade name for a pickling additive produced by Turco Products, Inc.

COATING DEVELOPMENT

The initial phase of the investigation was concerned with various methods of applying the barrier layer to chromium and the subsequent application of the external layer. The results of this work provided the basis for the selection of the systems which were evaluated.

Three techiques, electrodeposition, plasma spray and slurry-sinter were investigated as the means of forming the intermediate barrier sink layers. Two barrier layer compositions were prepared. One of these contained nominally six weight percent MgO, the other twelve weight percent MgO. Plasma spray and slurry sinter techniques were also used to investigate the formation of Kanthal external coatings. The barrier layers were titanized and silicided using a vacuum-pack cementation technique. Work on the different methods of forming barrier layers and external coatings was done concurrently.

Development of Intermediate Iron-MgO and Chromium-MgO Barrier Layers

Electroplating

Electroplating was the first method, examined as a means for depositing the iron-MgO and chromium-MgO barrier layers. For this work, 2-5 micron MgO particles were added to conventional iron (10) and chromium electroplating baths (11) having compositions given in Table V. It was not possible to form plates containing MgO particles from either of these plating baths, since the acidic bath reacted with the basic MgO to form a thick sludge from which the particles could not be deposited. However, in the absence of MgO both iron and chromium were successfully plated onto the Cr-5W-0.1Y alloy, although iron plating required a prior nickel strike.

Plasma Spray

Plasma spray techniques were also investigated as a means of forming intermediate layers on 0.50 inch (12.5mm) X 0.50 inch (12.5mm) Cr-5W-0.1Y specimens. The spraying parameters are given in Table VI. In some cases, the as-sprayed iron MgO coating was black or dark gray with regions of red coloration. A photograph and photomicrograph of the coatings are shown in Figures 1 and 2. The coatings appeared to be dense and adhered to the substrate. Attempts were made to exclude air from the region of the coupon by blanketing with flowing argon, but these attempts were unsuccessful. In order to reduce the oxidized regions and to remove the oxide film associated with the as-received powders, the coupons were heated in a tungsten boat in a purified hydrogen atmosphere. After the hydrogen treatment the iron-MgO coatings had a cracked, mosaic appearance of poor bonding as shown in Figure 3. Attempts were made to eliminate this cracking by heating the

plasma sprayed coatings for as long as 10 hours at 2200°F (1477°K). None of the times and temperatures investigated eliminated cracking. As a result no further work was done using plasma spraying as a means of depositing iron-MgO intermediate layers.

A typical plasma sprayed chromium-12 MgO coating had an appearance similar to the iron-MgO coated coupon shown in Figure 3 , except for the green oxide Cr_2O_3 which partially covered the surface. The microstructure of the as-sprayed coating is shown in Figure 4. The chromium-MgO coated coupons were treated in a hydrogen atmosphere to reduce Cr_2O_3. A series of heat treatments was performed in which the times ranged from one to five hours and temperatures from 1800°F (1255°K) to 2500°F (1588°K). Based on examination of microstructures such as shown in Figure 5, these hydrogen exposures only partially reduced the oxide, leaving an unreduced layer adjacent to the substrate. The plasma spray technique also produced large regions of MgO at the surface on which an adherent titanium coating could not be formed. For these reasons, plasma spray was abandoned as a means of forming the intermediate barrier layers for evaluation samples.

Slurry-Sinter

Slurry-sinter techniques (12) were also investigated as a means for forming both types of intermediate layers. A slurry was prepared by mixing 100 gm of the appropriate metal-oxide mixture with 120 ml cellulose nitrate. This mixture was sprayed onto the test specimen to form a layer approximately 0.004 inch (0.1mm) thick which was air dried at 100°F (311°K). After drying, the coupons were placed into a covered tungsten boat and sintered in a hydrogen atmosphere to densify and bond the coating to the substrate. The inlet hydrogen had a dew point of -78°F (212°K) and an exit dew point of -38°F (234°K).

Several different heating cycles were investigated to form the iron-MgO barrier layer. In each case a slow rise time of four to six hours to sintering temperature was used with the following sintering conditions:

Temperature °F	Temperature °K	Time Hours
1600	1144	1
1800	1255	1, 5, 8
2000	1366	5
2400	1588	1, 2

Although the iron particles sintered to form a ductile crack-free coating, a completely adherent bond could not be formed with the substrate. Figure 6

is a typical example of the lack of adherence observed with this coating. The poor adherence of the coating is believed to be due to the difference between the sinterability and coefficients of thermal expansion of iron and chromium. The values of these coefficients (16,17) are given below:

	°F	°K	α X10^{-6} in/in/°F
α-Fe	32-1472	273-1745	148
γ-Fe	1660-2530	1189-1661	23.0
Cr	1292	973	9.0

Because of the results obtained, addtional work on iron-slurry coatings was not undertaken.

The slurry-sinter technique was also used to form coatings of chromium-MgO. The sample preparation and coating application techniques were similar to those used for the iron-MgO system. Figure 7 shows a photomicrograph of the chromium-12MgO coating including electron microprobe analyzer (EMP) scans of the distribution of chromium and magnesium. The coatings were not always completly reduced, indicating that the hydrogen atmosphere had a varying degree of purity. This problem was eliminated by using a porous Al_2O_3 boat and completely surrounding the sprayed coupon with 50Cr-50Ti granules which acted as a getter. The boat was then placed into the cold zone of the hydrogen furnace. The furnace was evacuated to a pressure of 50 torr backfilled with high purity argon and purged for 15 minutes. This cycle was repeated and purified hydrogen was then passed into the furnace. After a hydrogen flame had been established at the furnace exit, the boat was gradually pushed into the hot zone at 2400°F (1588°K) over a period of two hours, held at temperature for two hours, immediately pushed into the cold zone and removed from the furnace. The resulting coatings were free of oxide and were bonded. Since this method of depositing an intermediate layer appeared promising, it was used in subsequent work.

Electrophoretic Deposition

As a modification of the slurry-sinter process, intermediate barrier layers were also deposited by electrophoretic techniques. The methods were an adaptation of procedures described by Ortner and Gebler (18). The dispersion suspending vehicle was a mixture of 1.1 parts nitromethane and one part anhydrous isopropanol. The solid content of the dispersion was a mixture of chromium + MgO having a concentration of 50 g/l. Cobaltous nitrate (0.12g/l) was added to the dispersion as an activator to increase the deposition rate and a small amount of zein (0.48g/l) (corn protein) was added to increase the green strength of the deposit. The specimen to be coated

was the cathode in the bath which was operated at room temperature. The anode was a 20 mesh Monel screen formed to provide an interelectrode spacing of 0.75 inch (1.9mm). Electrodes were also placed 0.75 inch (1.9mm) from the bottom and top edge of the coupon. The mixture was agitated to prevent settling of the particles. Coatings 0.003 inch (0.076mm) thick were deposited in one minute at 75 volts. These coatings which were sprayed with an acrylic plastic to permit handling prior to sintering in hydrogen for two hours at 2400°F (1588°K). These had a more uniform thickness than coatings formed by the slurry-sinter techniques. In other respects, the electrophoretic and slurry-sinter chromium-MgO barrier layers appeared to be identical. Figure 8 shows a photomicrograph and electron microprobe analyzer raster scans of a typical electrophoretic chromium-MgO coating. Because of the previously described difficulties, iron-MgO barriers were not deposited using the electrophoretic technique.

Development of Intermediate Chromium-Yttrium-MgO Barrier Layers

Work on development of chromium-yttrium-MgO barrier layers was essentially the same as for the chromium-MgO layer. The layers were deposited by slurry-sinter and electrophoretic techniques. The as-deposited layers were placed in porous alumina boats, completely surrounded by 50Cr-50Ti granules and sintered in hydrogen at atmospheric pressure. The inlet dew point was -78°F (212°K) and the exit dew point was -38°F (234°K). After 2 hours at 2800°F (1811°K) the barrier layer had volatilized leaving an uncoated substrate, while after 2 hours at 2600°F (1700°K) or 2 hours at 2400°F (1588°K) the coatings were sufficiently adherent to be handled but could be scraped from the surface. The inability to sinter the chromium-yttrium powder is attributed to the presence of yttrium oxide which was not reduced with hydrogen under the experimental conditions used (19).

Development of External Oxidation Resistant Coatings

Kanthal Coatings

Kanthal coatings 0.003 inch (0.076mm) thick were plasma sprayed, slurry-sinter or electrophoretically deposited on Cr-5W-0.1Y or Cr-7Mo-2Ta specimens and sintered for one or two hours in hydrogen using the techniques and appropriate coating formation parameters previously described. Two sintering temperatures, 2400°F and 2600°F (1588°K and 1700°K) were investigated using a five hour rise time to each temperature. Plasma spraying produced an adherent coating, which after hydrogen sintering, was excessively porous. Slurry-sinter and electrophoretic coatings showed deep cracks extending to the chromium alloy substrate. Adherent crack-free coatings were formed by repeated spraying and subsequently sintering

0.006 (0.15mm) thick layers for two hours at 2400°F (1588°K) in atmospheric hydrogen using a 50Cr-50Ti getter sealed retort. Preliminary oxidation exposure of these coatings for 2.75 hours at 2100°F (1422°K) prduced a green oxide and a weight gain of 9.7 mg/cm^2, indicating that the coating was not protective. After the same exposure conditions, a Kanthal rod was covered with a white oxide (Al_2O_3).

Since adherent iron-MgO intermediate layers could not be formed, the applicability of Kanthal to the chromium-MgO layers was considered. Intermediate chromium-MgO layers formed by plasma-spray and slurry-sinter were coated with a Kanthal slurry, sintered in hydrogen for 1 hour at 2400°F (1588°K) and static oxidation tested at 2100°F (1422°K). The results after 64 hours exposure are summarized below:

Intermediate Coating Method Cr+MgO	Total Weight Change mg/cm^2	Appearance
Plasma spray	-3	Spalled coating
Plasma spray	+7	Spalled coating
Slurry spray-sinter	+4	Green oxide

In view of these unfavorable results, no further work was done with the Kanthal system.

Titanizing and Siliciding Cr-7Mo-2Ta

Work on the development of parameters for titanizing Cr-7Mo-2Ta is summarized in Table VII. The coating from run 1 was not in the desired 6-10 mg/cm^2 range and was not evaluated further. The subsequent runs were made to evaluate the effects of varying coating parameters on the ability of the titanized layer to be silicided.

The siliciding work is summarized in Table VIII. The first run resulted in a blistered coating indicating that the titanized layer, which had not been annealed, could not be silicided under these conditions. Run 2 showed that less vigorous siliciding conditions still resulted in blistering. This blistering was similar to the wrinkling previously observed by Solar (5) under Contract NAS 3-7266. The problem was eliminated by annealing for four hours at 2400°F (1588°K) in an argon atmosphere at 150 torr. These titanizing and siliciding runs were used to select the coating parameters for preparing base-line oxidation test specimens (i.e., with no barrier layer).

Titanizing and Siliciding of Chromium-MgO and Chromium-Yttrium-MgO Barrier Layers

Work on titanizing and siliciding the chromium-MgO barrier layers was done using both alloy substrates. The results of titanizing and siliciding experiments on chromium-MgO intermediate layers are given in Table IX. The titanium coating had a satisfactory surface appearance, except for a slight sintering of pack particles to the coating. These particles were readily removed by gentle scraping. The siliciding of this coating (run 1 Table X) was not successful because of blistering and sintering of silicon pack particles to the coating. A second titanizing run using the parameters and heat treatments developed for coating Cr-7Mo-2Ta without the barrier layer, yielded a coating having a smooth metallic appearance and a weight gain comparable to that obtained on the Cr-7Mo-2Ta substrate. When the coating was silicided (run 2 Table X) using the parameters for Cr-7Mo-2Ta, the silicided coating was equivalent to that obtained on Cr-7Mo-2Ta. However, the coatings spalled suggesting that too much silicon was being deposited. This problem was solved by using a silicon pack diluted with -325 mesh Al_2O_3 in the ratio of one part silicon to three parts Al_2O_3 as shown in run 3 Table X.

COATING SYSTEMS SELECTED FOR EVALUATION

Based on the preceding coating development activities, the following six systems were selected for evaluation using Cr-7Mo-2Ta substrate:

Intermediate Barrier Layer	External Layer
Cr-6v/o MgO	Cr-Ti-Si
Cr-12v/o MgO	Cr-Ti-Si
Cr-Y-6v/o MgO	Cr-Ti-Si
Cr-Y-12v/o MgO	Cr-Ti-Si
None	Cr-Ti-Si (light)*
None	Cr-Ti-Si (heavy)

The barrier layers were formed by slurry-sinter and electrophoretic deposition. The specimens were placed in a porous Al_2O_3 boat, surrounded by granular 50Cr-50Ti and the layers were sintered in flowing hydrogen at atmospheric pressure for 2 hours at 2400°F (1588°K). Adherent chromium-MgO barriers were formed; however, the chromium-yttrium-MgO barriers were considerably less adherent. Both types of barrier layer coatings were diffusion annealed in an atmosphere of 150 torr argon for four hours at 2400°F (1588°K) then titanized and silicided using the parameters given in Tables XI, XII and XIII. After titanizing, the specimens were heat treated four hours at 2400°F (1588°K) before siliciding. In order to silicide the heavy coated specimens without causing the coating to spall, it was necessary to use a diluted pack with an Al_2O_3:Si ratio of 3:1. The coating weight associated with each of these sytems are summarized in the third, fourth and fifth columns of Table XIV.

---

* The light coating was 5.5 mg/cm^2 Ti and 14.7 mg/cm^2 silicon.

The heavy coating was 11.6 mg/cm^2 Ti and 12.1 mg/cm^2 silicon.

RESULTS OF COATING SYSTEMS EVALUATION

The following evaluation tests were made on Cr-7Mo-2Ta in the uncoated condition and after coating with the six systems previously described:

1) resistance to cyclic air oxidation at 2100°F (1422°K),
2) nitrogen contamination in the substrate during oxidation,
3) bend ductility transition temperature,
4) chemical composition of the surface oxidation products of coated and uncoated specimens,
5) metallographic examination of the coating and substrate before and after oxidation exposure,
6) the extent of interdiffusion associated with the oxidation exposure.

Oxidation Tests

Specimens of the six coating systems and uncoated Cr-7Mo-2Ta were cyclic oxidation tested at 2100°F (1422°K) in air for 200 hours. The weight change results are presented in Table XIV. Several of the coating systems exhibited essentially equivalent weight gains. The average weight change values, grouped according to coating systems which showed equivalent weight changes, are summarized in Figure 9.

Uncoated specimens exhibited weight gains for the first 100 hours exposure, then severely spalled during the next 20 hour increment and continued to spall at a less catastrophic rate for the remaining 80 hours exposure. All of the barrier layer specimens showed some degree of spalling (Table XIV), and there were no major differences in the performance of systems attributable either to the use of yttrium or different amounts of MgO in the preparation of the coating systems. In general the coating systems having electrophoretically deposited barrier layers exhibited lower weight gains than systems having slurry-sinter barrier layers. The Cr-Ti-Si base line systems exhibited the lowest average weight change after 200 hours exposure, with the light system having greater spalling and a slightly higher average weight gain than the heavy system. Figure 10 shows the appearance of representative specimens from each coating system after 200 hours exposure.

Nitrogen Contamination in Cr-7Mo-2Ta Substrate

After oxidation testing for 100 and 200 hours, specimens were removed from test for nitrogen analysis. The surface oxidation products and coating were removed from a sample of the oxidation test specimen by acid

etching. Although the acid reagent did not react with the substrate alloy, it did react with the diffusion zone immediately beneath the coating so that the samples submitted for analysis were about 0.001 inch (0.025mm) thinner per side than as-received. The nitrogen determinations were made using a micro-Kjeldhal technique and the results are summarized in Table XV. The compositions reported represent the total nitrogen content of the sample, i.e., the amount of nitrogen originally present in the alloy plus the amount of contamination after air exposure. Because the sample was dissolved during analysis, the values are average for the entire sample.

Bend Transition Temperature Testing

After 100 and 200 hours oxidation exposure at 2100°F (1420°K) in air, one specimen from each coating system was subjected to DBTT bend testing. All of the oxidized specimens were brittle at 1420 to 1490°F, (1055 to 1083°K). However, the alloy specimens as-received from NASA were ductile at 1090°F (861°K), which was the lowest temperature used for making bend tests. This ductility was expected since the alloy producer (8) reported a transition temperature of 548°F (560°K). In an effort to determine whether the embrittlement was produced by the heat treatment or nitrogen contamination, an uncoated specimen was subjected to the thermal cycle used to form the Cr-Ti-Si (light coating) at a pressure of 150 torr argon in a 50Cr-50Ti getter sealed retort. This specimen was brittle at 1490°F (1083°K) as was a Cr-Ti-Si (light) coated specimen. The appearance of these specimens after testing is shown in Figure 11. Specimen of the Cr-Ti-Si (heavy) coating as well as each of the four barrier layer systems were also brittle at 1490°F (1083°K). The post test appearance of the fractures in these specimens was similar to the specimens shown in Figure 11.

Chemical Composition of the Surface Oxidation Products

After oxidation exposure, the composition of the surface oxidation products for each of the systems investigated was determined by X-ray diffraction analysis. Table XVI summarizes the results for all specimens after 200 hours exposure, except for Cr-Ti-Si (light) which was evaluated after 100 hours exposure. The compositions of the oxides were obtained by comparison of the experimentally observed d-spacing with tabulated values(20). In addition to the compounds identified, other unidentified peaks were observed which may be complex silicides, oxides or silicates not catalogued. The only oxide detected on uncoated Cr-7Mo-2Ta was Cr_2O_3. All of the coating systems lines were indexed for Cr_2O_3 and in some cases TiO_2. No general correlation was apparent for the appearance of TiO_2. For future reference, the d-spacings and peak heights used in this analysis are compiled in Appendix 1 to this report.

Metallographic and Electron Microprobe Examination of the Coating Systems

Microstructural examinations were made on the as-received uncoated alloy also after 200 hours oxidation exposure at 2100°F (1422°K). Three coating systems having the lowest weight gains after 200 hours oxidation at 2100°F (1422°K) were selected for comprehensive evaluation. These were: Cr-Ti-Si (light), Cr-Ti-Si (heavy) and Cr-12 MgO/Cr-Ti-Si in which the Cr-MgO layer was electrophoretically deposited. Only one barrier system was evaluated because of the essential similarities among all of the barrier layer systems.

Figure 12 summarizes the light microscopy and EMP X-ray images obtained for the as-received Cr-7Mo-2Ta alloy. The average KHN of the alloy was 389. Metallographic examination of the alloy revealed the presence of two segregated phases. From the EMP examination of the alloy, it was found that chromium and molybdenum were uniformly distributed throughout the alloy, (Figure 12 c,d), as would be expected from a single phase solid solution and that tantalum (Figure 12e) was segregated. Yttrium (Figure 12f) was also segregated and the particles were elongated in the rolling direction of the alloy. Although it could not be shown by an X-ray scan, local examination revealed that oxygen was associated with the yttrium segregates.

Figure 13 presents KHN values of the indentations found in a specimen of the uncoated alloy after 200 hours exposure to 2100°F (1422°K) air. The absence of intergranular nitride precipitates, the low hardness toward the center of the specimens indicate that nitrogen has not been concentrated at the surface. An EMP scan confirmed the absence of a nitrogen gradient. The large grain boundary segregates in the region near the center of the photomicrograph were not identified.

Figure 14 shows a photomicrograph of another region in the oxidized uncoated alloy and also presents EMP images for the same region.* The chromium X-ray photograph (Figure 14c) qualitatively shows a gradual depletion in concentration from the matrix to the oxide surface. The oxygen X-ray image (Figure 14d) corroborates the X-ray diffraction results which show Cr_2O_3 at the specimen surface. There is also an apparent concentration of molybdenum (Figure 14e) at the oxide-substrate interface. The extent of the segregation of tantalum (Figure 14f) and yttrium (Figure 14g) was not changed by oxidation exposure and local EMP examination again revealed that oxygen was associated with yttrium.

Figure 15 presents the photomicrographs and microhardness traverses of the Cr-Ti-Si (light) coating system in the as-coated condition and after 100 hours exposure to air at 2100°F (1422°K). Figure 16 shows the EMP scans of the same specimens.

* In Figures 14, 16, 18 and 20 the EMP X-ray photomicrographs are direct reproductions, whereas the optical photomicrographs are mirror images of the regions photographed. This inversion of images is caused by differences in the optical systems of the EMP and the metallograph used to examine the specimens.

In the as-coated condition, the coating system was characterized by a sharp interface between the coating and the coated substrate (Figure 15a). Approximately in the middle of the coating layer there is a region, which appears as a spotty zone on the photomicrograph (Figure 15a) but the EMP electron absorption image (Figure 16c) showed it to have a definite structure. In the coating, chromium (Figure 16e) and tantalum concentrations (Figure 16i) gradually decreased away from the coating-substrate interface and the concentration of molybdenum (Figure 16f) decreased abruptly at the coating-substrate interface. The presence of tantalum and molybdenum in the coating indicated that these elements diffused from the substrate during the formation of the coating. The concentrations of titanium (Figure 16j) and silicon (Figure 16m) are highest at the external surface of the coating. Beneath these external zones, there is a region in which the concentrations of these elements are lower, but essentially uniform. Titanium and silicon did not penetrate from the coating into the substrate.

After 100 hours of cyclic oxidation exposure, a diffusion zone (Figures 15b, 16b) had formed between the coating and the substrate. This diffusion zone was characterized by high hardness. The relative intensities of the X-ray images indicated that the diffusion zone did not act as a barrier to the outward diffusion of chromium (Figure 16g) or molybdenum (Figure 16h). Tantalum segregation (Figure 16k) was observed at the diffusion zone-substrate interface. The intensity of the respective X-ray images indicated that titanium (Figure 16l) had not penetrated into the coating as far as the diffusion zone and that silicon (Figure 16o) penetrated further than titanium and into the diffusion zone. No evidence of nitrogen contamination of either the as-coated or the oxidation tested substrates was found by microhardness measurement and EMP analyses.

Figure 17 shows photomicrographs and microhardness data for the Cr-Ti-Si (heavy) system as coated, and after 100 and after 200 hours oxidation exposure at 2100°F (1422°K). The essential features of the coating are the same as for the Cr-Ti-Si (light) system; i.e., a hard coating with an internal structure. The differences in the appearance of the interface regions are artifacts attributed to variability in the etching characteristics rather than to changes resulting from thermal exposure.

The EMP photographs of the as-coated specimens presented in Figure 18 shows that in the coating the concentrations of chromium (Figure 18e) and tantalum (Figure 18i) gradually decrease away from the coating-substrate interface. Comparison of Figures 18k and 18m shows that for this

specimen titanium (Figure 18k) penetrated further than silicon (Figure 18m). Yttrium (Figure 18o) was again present as segregated particles. Aluminum (Figure 18q) and oxygen (Figure 18s) were detected at the outer surface of the coating. The source of these elements was the Al_2O_3 diluent used during the siliciding step.

After 200 hours oxidation exposure chromium (Figure 18f) had diffused to the coating surface, gradually decreased in concentration from the substrate to the coating surface and was depleted at the coating substrate interface. The concentration of molybdenum (Figure 18h) gradually decreased towards the coating surface and there was also evidence of depletion at the coating substrate interface. This coating-substrate interface region was enriched in tantalum (Figure 18j). The coating-substrate interface also appeared depleted in titanium, and titanium also penetrated into the substrate (Figure 18l). The penetration of silicon (Figure 18n) into the substrate was less pronounced than titanium and not as far beyond the coating-substrate interface. No aluminum was detected at the surface (Figure 18r), possible due to the spalling of the outer coating layer during oxidation. Oxygen (Figure 18t) was found to be associated with the chromium and titanium at the outer surface of the coating.

Figure 19 shows photomicrographs and microhardness traverses through the coating and substrate for the Cr-12MgO/Cr-Ti-Si coating system as-coated, after 100 hours, and 200 hours air oxidation exposure at 2100°F (1422°K). The region between the dense outer coating and the alloy substrate contained considerable porosity, which may have been caused by an instability of MgO during the coating formation cycle. There is also a relatively hard zone in the center of the coating which persisted throughout the exposure life of the coating. This region was softer than the corresponding regions in the Cr-Ti-Si systems, (Figures 15 and 17). There was also a relatively soft outer surface region similar to that formed on the Cr-Ti-Si (heavy) system (Figure 17). The high microhardness value in the substrate immediately below the coating suggests nitrogen comtamination. However, nitride precipitates were not metallographically detected in the portion of the specimen examined.

Figure 20 presents the EMP images of the specimen in the as-coated condition and after 200 hours air oxidation exposure. In the as-coated condition, there was a chromium concentration gradient (Figure 20e) in the coating through the silicided region (Figure 20m) of the coating. The barrier layer did not prevent the outward diffusion of either molybdenum (Figure 20g) or tantalum (Figure 20i) from the substrate. Titanium (Figure 20k) penetrated slightly into the substrate and the titanized region of the coating was not completely silicided (Figure 20m).

After 200 hours cyclic oxidation at 2100°F (1422°k) there was evidence of chromium diffusion outward into the coating layer. However, the outward diffusion of molybdenum (Figure 20h) was restricted to the barrier layer region. The barrier did not limit the outward diffusion of tantalum (Figure 20j). However, there was evidence of segregation near the barrier-substrate interface which was also the limit of titanium penetration (Figure 20l). Yttrium was again segregated in the coating layers (Figure 20p). As previously found for coatings which were silicided in a pack diluted with Al_2O_3, aluminum (Figure 20q,r) and oxygen (Figure 20s,t) were detected at the outer surface of the coating.

DISCUSSION OF RESULTS

Three coating systems were investigated for use as a means of protecting Cr-7Mo-2Ta-0.09C-0.1Y against oxidation and nitrogen contamination from 2100°F (1422°K) air. One of these was a titanium-modified chromium silicide formed directly on the chromium alloy. The other two were barrier layer systems. In conceptual form each barrier layer system consisted of two layers; an oxidation resistant exterior Cr-Ti-Si coating and, an intermediate layer formed directly on the chromium alloy substrate. Two intermediate layers were ivestigated. One of these consisted of a chromium layer in which MgO particles were dispersed, the other was a prealloyed chromium-yttrium layer also containing MgO particles. The nominal MgO content of these systems was either 6 or 12 volume percent. Since the oxidation performance and the microscopic appearance of all four barrier layer systems were essentially the same, only the Cr-12MgO/Cr-Ti-Si system was characterized by metallographic analysis.

As shown in Table XIV and Figure 9, all six of the coating systems had lower oxidation weight changes than uncoated Cr-7Mo-2Ta alloy. Approximately equivalent weight gains were found for coatings which used either unalloyed chromium or prealloyed chromium-yttrium powders. Lower oxidation weight gains for electrophoretically deposited barrier layers are attributed to the formation of a more dense and more uniform barrier layer than was formed by slurry-spray techniques. Oxidation weight gains for all four of the barrier layer coatings systems were higher than for the Cr-Ti-Si(light) and Cr-Ti-Si(heavy) coating. This result was obtained because the Cr-Ti-Si layer on the barrier coating systems was not modified by the presence of molybdenum or tantalum, whereas the Cr-Ti-Si(light) and Cr-Ti-Si(heavy) coatings formed directly on the Cr-7Mo-2Ta substrate contained these modifying elements which improved oxidation resistance. The weight gain found for the Cr-Ti-Si(heavy) coating was slightly lower(and the time-weight gain curve more uniform) than for the Cr-Ti-Si(light) coating. The Cr-Ti-Si(heavy) coating was silicided using a pack which was diluted with Al_2O_3. Aluminum and oxygen were found at the surface of the coating by EMP examination and the improved oxidation resistance is attributed to the presence of Al_2O_3 at the coating surface.

After completion of the barrier deposition and Cr-Ti-Si coating process, no MgO particles were metallographically detected in the barrier layer. EMP raster scans from the external coating surface into the substrate showed no significant radiation from magnesium. Consequently, a magnesium X-ray photograph was not included in Figure 20. Photomicrographs of the coating (Figure 19a, 20a) showed a porous, structured region immediately above the substrate. It is suggested that this was the region which contained MgO and that the oxide was unstable during the titanizing step of coating process (Figure 20b).

The bend transition temperature of the substrate was raised by the coating process. This may be attributed to several factors acting either singly or in combination. Titanium or silicon penetration into the substrate may have produced embrittlement. However, this does not seem likely based on the work of Stephens and Klopp (6) which showed that titanium and silicon coatings did not embrittle Cr-0.17Y or Cr-5W-0.18Y. Nitrogen contamination, with consequent embrittlement, may have occurred during titanizing or siliciding, since the Cr-Ti powder used for the getter seals, as well as for titanizing the substrates contained about 0.045 weight percent nitrogen (See Table 3). Evolution of this nitrogen during the titanizing step, or in the case of the barrier layer systems during the sintering step may have resulted in nitrogen contamination of the substrate. The thermal treatments used either to sinter the barrier layers or to diffusion anneal the titanized coating layer could also have caused embrittlement since a comparable thermal treatment on an uncoated specimen produced a similar increase in the DBTT.

The development of useful coatings for chromium base alloys will be dependent on attaining protective coatings from processing treatments which do not depend on coating cycles that can significantly degrade the mechanical properties of the substrate material.

CONCLUSIONS

Based on the experimental data from this program, the following conclusions were made.

1. Because of the relatively high (>1490°F (1055°K) ductile-to brittle bend transition temperature of the coated substrate, the coatings evaluated were not considered usable as protective systems for advanced turbine components.

2. Although nitrogen contamination could be a contributing factor, the relatively high ductile-to-brittle bend transition temperature was attributed to the effect of thermal treatment during the coating process.

3. After oxidation testing, total nitrogen content in the substrate was essentially the same for each coating. After testing in air at 2100°F the nitrogen content was typically 0.008 weight percent after 100 hours and 0.01 weight percent after 200 hours cyclic testing compared to 0.0022 weight percent initially present in the Cr-7Mo-2Ta.

4. Based on weight gain measurements after cyclic oxidation testing in air at 2100°F (1422°K) for 200 hours, the order of increasing weight gain; i.e., decreasing protection, provided by the six coating systems was:

    1. Cr-Ti-Si (heavy)
    2. Cr-Ti-Si (light)
    3. Cr-Y-12 MgO (slurry), Cr-Y-12 MgO (electrophoretic), Cr-Y-6 and 12 MgO (electrophoretic), Cr-6 and-12 MgO (electrophoretic
    4. Cr-6 and -12 MgO (slurry)

5. Metallographic examination of the MgO barrier layer coatings as-formed and after 100 and 200 hours of oxidation testing, revealed a region of porosity which was believed to have resulted from some chemical instability of the MgO particles associated with the coating formation process.

9. REFERENCES

1. Clark, J.W., "Development of High-Temperature Chromium Alloys", General Electric Company (NASA CR-92691), June 30, 1967.

2. Henderson, F., Johnstone, S.T.M., and Wain, H.L., "The Effect of Nitride-Formers Upon the Ductile-Brittle Transition in Chromium", J. Inst. Metals, Vol. 92, 1963-64, pp. 111,117.

3. Williams, D.N., Ernest, R.H., MacMillan, C.A., English, J.J., and Bartlett, E.S., "Development of Protective Coating for Chromium-Base Alloys", Battelle Memorial Inst. (NASA CR-54619), March 5, 1968.

4. Negrin, Marvin, and Block, Allan, "Protective Coatings for Chromium Alloys", Chromalloy American Corporation (NASA CR-54538), July 13, 1967.

5. Brentnall, W.D., Shoemaker, H.E., and Stetson, A.R. "Protective Coatings for Chromium Alloys", Rep. RDR-1398-2, Solar Div., International Harvester (NASA CR-54535), August 20, 1966.

6. Stephens, J.R., and Klopp, W.D., "Exploratory Study of Silicide, Aluminide and Boride Coatings for Nitridation-Oxidation Protection of Chromium Alloys", (NASA TN D-5157), April 1969.

7. Goetz, L.J., Hughes, J.R., and Moore, W.F., "The Pilot Production and Evaluation of Chromium Alloy Sheet and Plate", Lamp Metals and Components Department, General Electric Company (NASA CR-71284), March 15, 1967.

8. Slaughter, E.R., Hughes, J.R. and More, W.R., "Small Quantity Production of Complex Chromium Alloy Sheet", Lamp Metals and Components Department, General Electric Company (NASA CR-72545), December 1968.

9. Refractory Metals Sheet Rolling Panel, Evaluation Test Methods for Refractory Metal Sheet Material", Materials Advisory Board, National Academy of Science, Washington, D.C. (Report MAB 192-M), April 22, 1963.

10. Metal Finishing Guide Book, 37th Edition, Metals and Plastics Publications, Inc., 1968, p. 247.

11. Operating Instructions for Diamond GPA 1800, Chromium Metals Division, Diamond Alkali Company, no date.

12. Gadd, J.D., Fisch, H.A., Kmiecíak, H.A., and Jones, E.E., "Vacuum Pack and Slip-Pack Processes for Coating Refractory Metals", Electrochem Tech., Vol. 6, No. 11-12, November-December 1968, pp. 379-389.

13. American Society for Metals, Metals Handbook, Eighth Edition, Vol. 2, 1963, p. 83.

REFERENCES (Cont'd)

14. ibid. Vol. I, 1961, p. 1212.

15. ibid. Vol. I, 1961, p. 1201.

16. ibid. Vol. I, 1961, p. 1207.

17. Smithells, Colin J., Metals Reference Book, Third Edition, Vol. 2, Butterworths, 1962, p. 696.

18. Ortner, Martin H., and Gebler, Kenneth A., "Electrophoretic Deposition of Refractory Metals Coatings", Vitro Laboratories (USAF-ML-TR-68-24) February, 1968.

19. Kubaschewski, O. and Hopkins, B. E., "Oxidation of Metals and Alloys", 2nd Edition, Academic Press, 1962, pp. 8, 9.

20. "Inorganic Index to the Powder Diffraction File", ASTM Publication PD-IS-171, 1967.

TABLE I. - AVERAGE COMPOSITION OF CHROMIUM-BASE ALLOYS
(WEIGHT PERCENT (REFS. 7 and 8)

	Cr-5W-0.1Y		Cr-7Mo-2Ta			
	Heat 84-100		Heat 140-100		Heat 131-100	
Element	Ingot	Sheet	Ingot*	Sheet	Ingot*	Sheet
Cr						
W	4.93	5.02	<0.05/ 0.05		<0.05/ 0.05	
Y	0.19	0.18	0.14/0.21		0.07/0.11	
Mo			7.09/7.15		6.97/7.05	
Ta			2.11/2.16		2.07/2.13	
C	0.003	0.0012	0.089/0.103	0.103	0.098/0.091	0.099
La			0.12/0.12		0.04/0.04	
O	0.0057	0.0095	0.0128/0.0136	0.0025 0.0036 0.0044	0.0049/0.0064	0.0049±5
N	0.0046	0.0024	0.0095/0.0087	0.0029 0.0028	0.0005/0.0006	0.0016±5
H	0.0007	0.0012	0.0014/0.0032	0.0033	0.0005/0.0006	0.0016±5
P	0.002	0.002	<0.002/<0.002	<0.002	<0.002/<0.002	<0.002
S	0.004	0.002	0.0027/0.0016	<0.001	0.0026/0.0023	<0.001
Al			0.002/0.002		0.007/0.007	
Fe			0.003/0.003		0.003/0.003	
Hf			<0.05/<0.05		<0.05/<0.05	
Cb			<0.03/<0,03		<0.03/<0.03	
Ni			<0.001/<0.001		<0.001/<0.001	
			0.01/0.01		0.02/0.02	
Ti			<0.001/<0.001		0.001/0.001	
V			<0.001/<0.001		<0.001/<0.001	
Zr			0.007/0.007		0.005/0.005	

* Top/Bottom analysis of ingot.

TABLE II. - COMPOSITION OF POWDERS USED TO FORM THE INTERMEDIATE COATING LAYERS (WEIGHT PERCENT)

Element	Material Composition				
	Cr	Cr-Y	MgO	Fe	Kanthal
Cr	99.2	99.66			25
Y		0.34[3]			
Mg	0.11[1]	<0.001	Bal.		
O	0.5				
Fe	0.075	0.01-0.1	0.01-0.1	99.9[2]	Bal.
Al	0.035	0.01-0.1	0.001-0.005		4
N	0.007	-			
S	0.003	-			
C	0.085	-	-		
Si		0.01-0.1	0.1-1.0		
Mn		<0.001	0.01-0.1		
Ni		0.01-0.001			
Cu		<0.001	0.001		
V			0.001-0.01		
Ti		<0.01			
B			0.05-0.5		
Ca			0.01-0.1		
Sn			0.001		
Pb			0.001		
Co					3
Nominal particle diameter, microns	10	2-10	2-5	3.0	0.68

(1) Reported as MgO

(2) Carbonyl iron, no other values reported

(3) Estimated by difference

TABLE III - COMPOSITION OF MATERIALS USED TO FORM THE TITANIZED AND SILICIDED COATING LAYERS (WEIGHT PERCENT)

Element	Material Composition		
	50Cr-50Ti	60Cr-40Ti	100Si
Cr	50.5	59.0	
Ti	49.2	40.6	
Fe	0.122	0.5	0.50
C	0.023	0.027	
N	0.0143	0.047	
O	0.13	0.049	
Si			98.67
Ca			0.07

TABLE IV.- ELECTROPOLISHING PROCEDURE USED TO PREPARE CHROMIUM SAMPLES

Material	Electrolyte for Cr-5W-0.1Y Weight percent	Electrolyte for Cr-7Mo-2Ta 0.09C-0.1Y Weight Percent
Concentrated Sulphuric Acid	60	60
85 percent Ortho Phosphoric Acid	20	20
Citric Acid	10	10
Water	10	10
Operating Conditions		
Current Density, amps/in^2	2.0	2.0
Temperature	120-130°F (322-327°K)	R.T.
Cathode Material	lead	lead

TABLE V.- COMPOSITION AND OPERATING CONDITIONS FOR ELECTROPLATING BATHS

	Composition oz/gal	
	Iron Bath	Chromium Bath
$FeSO_4 \cdot 7H_2O$	33	
$FeCl_2 \cdot 2H_2O$	4.8	
Nh_4Cl	2.7	
MgO, volume percent	0.6-2.8	0.6-2.8
Cr_2O_3		33.
SO_4		0.20
Additive *		1.18

	Operating Conditions	
	Iron Bath	Chromium Bath
Bath temperature	115°F (292°K)	115°F (292°K)
Current density	23 amp/ft^2	500 amp/ft^2
Anode	Lead	Lead

* Nitradd, Turco Products, Inc.

TABLE VI.- PLASMA SPRAYING PARAMETERS FOR INTERMEDIATE BARRIER LAYERS

	Fe	Cr	MgO	Fe+12MgO	Cr+12MgO
Powder Size, Microns	3	10	2-5	3+2-5	10+2-5
Arc Gas	Ar+H	Ar+H	Ar+H	Ar+H	Ar+H
Arc Gas Flow, Cu ft/hr	Ar+H	Ar+H	Ar+H	Ar+H	Ar+H
Argon	100	100	100	100	100
Hydrogen	3.5	3.5	3.5	3.5	3.5
Powder Gas	Ar	Ar	Ar	Ar	Ar
Powder Gas Flow ft/min.	40	40	40	40	40
Powder Feed Rate, gm/min.	3.5	3.7	1.7	4.0	313
Spraying Distance, in.	2.5	2.5	2.5	2.5	2.5
Arc Current, amps.	880	880	880	880	880
Arc Voltage, volts.	44	44	44	44	44

TABLE VII. - PARAMETERS FOR TITANIZING Cr-7Mo-2Ta ALLOY

Exp. No.	Pack Comp. w/o	Activator	Coating Formation Parameters				Coating Properties			Remarks
			Time hrs	Temp. °F	Temp. °K	Pressure torr	Average Buildup per side in	Average Buildup per side mm	Average Wt. Gain mg/cm^2	
1	60Cr-40Ti	1%NaF	6.0	2350	1561	150	-	-	4	
2	60Cr-40Ti	1%NaF	15.0	2350	1561	150	-	-	6.1	Used in silicide.Run 2
3	60Cr-40Ti	1%$CrCl_3$	8.0	2200	1477	150	-	-	7.5	Used in silicide.Run 3
4	50Cr-50Ti	1%NaF	5.0	2200	1477	150	-	-	8.4	Annealed 4 hr 2400°F and used in silicide. Run 3
5	50Cr-50Ti	1%NaF	10.0	2200	1477	1×10^{-4}	-	-	8.8	Used in silicide.Run 1
6	50Cr-50Ti	1%NaF	10.0	2200	1477	1×10^{-4}	0.0008	0.02	7.9	Diffusion annealed after coating.

TABLE VIII. - PARAMETERS FOR SILICIDING OF Cr-7Mo-2Ta ALLOY

Exp. No.	Pack Comp. w/o	Activator	Coating Formation Parameters				Coating Properties			Remarks
			Time hrs	Temp. °F	Temp. °K	Pressure torr	Average Buildup per side in	Average Buildup per side mm	Average Wt. Gain mg/cm^2	
1	100 Si	2%KF	2.5	2200	1366	150	-	-	-	Blistering and sintering on unannealed Cr-Ti substrate.
2	100 Si	1%KF	4.0	1800	1255	150	-	-	-	Blistering and sintering on unannealed Cr-Ti substrate.
3	100 Si	1%KF	3.0	1900	1311	150	-	-	-	Blistering and sintering on unannealed Cr-Ti substrate. Smooth coating on Cr-Ti annealed 4 hr (1588°K).
4	100 Si	1%KF	2.0	2000	1366	1×10^{-4}	0.0015	0.038	16.0	Smooth coating on Cr-Ti annealed 4 hr 2400°F (1588°K).

TABLE IX. - PARAMETERS FOR TITANIZING Cr-5W-0.1Y ALLOY HAVING CHROMIUM-MgO INTERMEDIATE LAYERS

Exp. No.	Pack Comp. w/o	Activator	Coating Formation Parameters: Time hrs	Temp. °F	Temp. °K	Pressure torr	Coating Properties: Average Buildup per side in	mm	Average Wt. Gain mg/cm^2	Remarks
1	50Cr-50Ti	0.5%$CrCl_3$	10.0	2200	1477	150	0.0015	0.038	26.2	Slight sintering
2	50Cr-50Ti	1%NaF	10.0	2200	1477	1×10^{-4}	-	-	7.4	Smooth coating

TABLE X. - PARAMETERS FOR SILICIDING CHROMIUM ALLOYS HAVING CHROMIUM-MgO INTERMEDIATE LAYERS

Exp. No.	Pack Comp. w/o	Activator	Coating Formation Parameters: Time hrs	Temp. °F	Temp. °K	Pressure torr	Coating Properties: Average Buildup per side in	mm	Average Wt. Gain mg/cm^2	Remarks
1	100 Si	1%KF	2.0	2000	1366	150	-	-	-	Coating blistered Cr-5W substrate.
2	100 Si	1%KF	2.0	2000	1366	1×10^{-4}	-	-	12.5	Smooth coating Cr-5W substrate
3	Al_2O_3:Si=3:1	1%KF	10.0	2000	1366	1×10^{-4}	0.003	0.076	19.5	Al_2O_3 diluent pack Smooth coating Cr-7Mo-2Ta substrate

TABLE XI - PARAMETERS FOR TITANIZING AND SILICIDING INTERMEDIATE BARRIER LAYERS ON Cr-7Mo-2Ta ALLOY

Coating Layer	Pack Comp. w/o	Activator	Time hrs.	Temperature °F	Temperature °K	Pressure Torr
Titanizing	50Cr-50Ti	1% NAF	10	2200	1477	1×10^{-4}
Siliciding	Al_2O_3:Si=3:1	1% KF	10	2000	1366	1×10^{-4}

TABLE XII - PARAMETERS USED FOR TITANIZING AND SILICIDING Cr-Ti-Si (light) COATING ON Cr-7Mo-2Ta ALLOY

Coating Layer	Pack Comp. w/o	Activator	Time hrs.	Temperature °F	Temperature °K	Pressure Torr
Titanizing	50Cr-50Ti	1% NAF	10	2200	1477	1×10^{-4}
Siliciding	100Si	1% KF	2	2000	1366	1×10^{-4}

TABLE XIII - PARAMETERS USED FOR TITANIZING AND SILICIDING Cr-Ti-Si (heavy) COATING ON Cr-7Mo-2Ta ALLOY

Coating Layer	Pack Comp. w/o	Activator	Time hrs.	Temperature °F	Temperature °K	Pressure Torr
Titanizing	50Cr-50Ti	1% NAF	10	2200	1477	150
Siliciding	Al_2O_3:Si=3:1	1% KF	10	2000	1366	1×10^{-4}

TABLE XIV. - NITRIDATION/OXIDATION WEIGHT CHANGE DATA

System or Barrier	Spec. No.	Coating Layer Mg/Cm² Barrier	Ti	Si	Total Weight Change (Mg/Cm²) At Indicated Time (Hours) 2	4	6	8	10	12	14	16	18	20	40	60	80	100	120	140	160	180	200
Cr-7Mo-2Ta	Cr1	-	-	-	0.32	0.74	0.82	0.96	1.28	1.38	1.49	1.67	1.77	1.84	2.52	2.98	3.37	3.72	-5.71	-6.56	-6.74	-6.91	-6.88
	Cr2	-	-	-	0.92	1.42	1.81	2.20	2.30	2.41	2.48	2.55	2.66	2.73	3.40	4.04	4.36	4.72	-3.09	-4.08	-4.22	-4.36	-4.22
	Cr3	-	-	-	0.85	1.21	1.38	1.63	1.77	1.95	2.09	2.38	2.52	2.59	3.30	3.76	4.18	4.65					
Cr-Ti-Si	1	-	5.7	13.3	0.74	0.99	1.03	1.06	1.13	1.13	1.17	1.20	1.17	1.20	1.28	1.42	1.56	1.67	2.76	2.94	2.98	2.87	2.87
LIGHT	3	-	5.5	16.1	0.67	0.92	0.92	0.96	1.06	1.06	1.06	1.10	1.13	1.17	1.35	1.56	1.77	1.95	2.76	2.84	2.70	2.62	2.48
	4	-	5.5	16.1	0.67	0.89	0.89	0.96	0.99	0.99	1.03	1.06	1.10	1.13	1.31	1.49	1.74	1.84					
	5	-	5.5	15.6	0.60	0.89	0.92	0.99	1.03	1.03	1.03	1.06	1.10	1.13	1.35	1.60	1.88	1.99	2.94	2.76	2.76	2.59	2.55
	6	-	5.5	14.1	0.60	0.85	0.89	0.99	0.99	1.03	1.03	1.10	1.13	1.16	1.28	1.38	1.60	1.70					
	7	-	5.6	13.7	0.67	0.89	0.99	0.99	1.10	1.06	1.06	1.10	1.17	1.20	1.31	1.38	1.60	1.67	2.62	2.70	2.73	2.59	2.62
	9	-	5.5	14.2	0.60	0.85	0.89	0.96	0.96	0.99	0.99	1.06	1.06	1.10	1.20	1.38	1.63	1.77					
Cr-Ti-Si	115-1	-	11.5	12.0	0.53	0.60	0.63	0.70	0.74	0.70	0.77	0.77	0.81	0.81	1.13	1.37	1.44	1.59	1.59	1.66	1.69	1.69	1.69
HEAVY	115-2	-	11.4	11.7	0.84	0.88	0.88	0.95	0.98	0.95	0.98	0.98	1.06	1.06	1.41	1.59	1.69	1.83	1.87	1.94	1.97	2.01	2.01
	115-3	-	12.0	12.7	0.84	0.88	0.91	0.95	0.98	0.95	1.02	1.02	1.06	1.06	1.27	1.90	2.12	2.26					
Cr-Y-12MgO	112-8	9.8	9.1	15.5	0.53	0.56	0.60	0.67	0.70	0.70	0.84	0.88	0.95	1.02	1.37	2.12	2.40	2.82	3.18	3.42	3.63	3.92	4.06
SLURRY	112-9	8.9	8.3	14.1	0.45	0.49	0.53	0.60	0.63	0.63	0.77	0.77	0.88	0.91	1.20	1.90	2.26	2.73	3.21	3.42	3.53	3.74	3.85
	112-10	9.7	8.9	15.3	0.42	0.49	0.49	0.56	0.60	0.67	0.77	0.81	0.9	0.95	1.30	2.44	2.80	3.15					
Cr-Y-12MgO	111-A	14.9	12.5	23.0	0.56	0.81	0.88	0.91	0.98	1.02	1.06	1.20	1.23	1.27	1.48	2.09	2.51	3.42					
ELECTRO	111-B	10.6	9.9	20.9	0.42	0.56	0.63	0.67	0.74	0.77	0.77	0.88	0.95	0.98	1.09	1.24	2.09	2.72	2.82	3.00	3.21	3.32	3.46
	111-C	10.7	11.1	20.9	0.38	0.56	0.67	0.70	0.74	0.81	0.84	0.95	1.02	1.06	1.20	1.80	2.26	3.03	3.21	3.42	3.64	3.78	3.95
Cr-Y-6MgO	111-D	5.6	7.7	19.1	0.45	0.63	0.70	0.74	0.77	0.81	0.88	0.95	1.02	1.06	1.27	1.87	2.19	2.47					
ELECTRO	111-E	6.4	7.5	18.8	0.35	0.49	0.56	0.60	0.63	0.70	0.74	0.81	0.88	0.91	1.06	1.56	2.02	2.33	2.57	2.75	2.89	3.00	3.07
	111-F	6.1	7.9	19.2	0.53	0.67	0.74	0.74	0.81	0.84	0.88	0.98	1.06	1.09	1.24	1.80	2.19	2.47	2.65	2.82	3.00	3.14	3.32
Cr-12 MgO	110-2	20.3	10.6	19.6	0.28		0.14	0.21	0.31	0.38	0.53	0.67	0.77	0.88	1.34	2.48	3.12	3.74	3.85	4.09	4.38	4.48	4.27
SLURRY	110-6	10.9	9.	23.9	0.21	0.53	0.67	0.70	0.74	0.88	0.88	0.95	0.98	1.02	1.23	2.54	3.07	3.43	3.81	4.06	4.31	4.62	4.86
	110-9	12.0	10.0	23.9	0.21	0.42	0.60	0.67	0.74	0.84	0.84	0.91	0.95	1.02	1.23	3.00	3.25	4.03					

TABLE XIV. - NITRIDATION/OXIDATION WEIGHT CHANGE DATA (Continued)

System or Barrier	Spec. No.	Coating Layer Mg/CM^2 Barrier	Ti	Si	Total Weight Change (Mg/Cm^2) At Indicated Time (Hours) 2	4	6	8	10	12	14	16	18	20	40	60	80	100	120	140	160	180	200
Cr-12MgO	111-G	26.7	12.6	16.5	0.42	0.53	0.70	0.77	0.84	0.98	0.98	1.02	1.06	1.13	1.27	2.12	2.12	2.36					
ELECTRO	111-H	26.7	12.6	13.7	0.42	0.53	0.60	0.67	0.77	0.88	0.88	0.92	0.95	1.02	1.20	2.04	2.44	2.72	2.93	3.11	3.39	3.67	3.86
	111-I	27.0	12.9	14.7	0.21	0.24	0.35	0.42	0.49	0.60	0.60	0.63	0.70	0.77	0.98	1.90	2.26	2.50	2.79	3.00	3.11	3.25	3.35
Cr-6MgO	110-1	18.1	9.6	15.5	0.24	0.60	0.77	0.88	1.09	1.20	1.37	1.59	1.69	1.83	2.55	3.75	4.43	4.84					
SLURRY	110-2	21.5	10.8	18.5	0.38	0.74	0.88	0.95	1.09	1.23	1.41	1.59	1.69	1.80	2.34	2.48	3.97	4.41	4.80	5.12	5.23	5.12	4.77
	110-3	16.9	9.6	17.0	0.38	0.70	0.84	0.91	1.02	1.09	1.20	1.34	1.44	1.55	1.95	2.76	3.33	3.81	4.27	4.55	4.70	4.77	4.56
Cr-6MgO	112-J	31.8	13.8	11.4	0.49	0.56	0.67	0.77	0.84	1.02	1.09	1.09	1.20	1.20	1.48	2.19	2.65	2.80	2.93	3.14	3.10	2.80	2.80
ELECTRO	112-K	32.0	14.0	10.4	0.49	0.56	0.67	0.77	0.84	0.95	0.98	1.02	1.13	1.13	1.48	1.98	2.12	2.02					
	112-L	31.0	14.3	11.5	0.32	0.39	0.49	0.60	0.67	0.77	0.84	0.91	0.98	1.02	1.41	1.84	2.22	2.48	2.65	2.75	2.86	2.93	2.86

TABLE XV - NITROGEN ANALYSIS OF SUBSTRATE AFTER AIR OXIDATION

EXPOSURE AT 2100°F (1422°K)

System or Barrier	Spec. No.	Coating Layer Mg/Cm^2 Barrier	Ti	Si	Wt. Change Mg/Cm^2	Total N_2 Contamination (Wt%) 0 hr	100 hr	200 hr
Cr-7Mo-2Ta	-	-	-	-	-	0.0022		
	Cr-3	-	-	-	+4.65		0.009	
	Cr-1	-			-6.88			0.010
Cr-Ti-Si(1)	9	-	5.5	16.1	+1.77		0.006	
Cr-Ti-Si(h)	3	-	12.0	12.7	+2.26		0.008	
	1	-	11.5	12.0	+1.69			0.0075
Cr-Y-12MgO(s)	112-10	9.7	8.9	15.3	+3.15		0.0085	
	112-8	9.8	9.1	15.5	+4.06			0.0095
Cr-Y-12MgO(e)	111-A	14.9	12.5	23.0	+3.42		0.007	
	111-B	10.0	9.9	20.9	+3.46			0.007
Cr-Y-6MgO(e)	111-D	5.6	7.7	19.1	+2.47		0.008	
	111-F	6.1	7.9	19.2	+3.32			0.0105
Cr-12MgO(s)	110-9	12.0	10.0	23.9	+4.03		0.007	
	110-6	10.9	9.4	23.9	+4.86			0.0087
Cr-12MgO(e)	111-G	26.7	12.6	16.5	+2.36		0.010	
	111-H	26.7	12.6	13.7	+3.86			0.007

TABLE XV - NITROGEN ANALYSIS OF SUBSTRATE AFTER AIR OXIDATION

EXPOSURE AT 2100°F (1422°K) - continued

System or Barrier	Spec. No.	Coating Layer Mg/Cm^2 Barrier	Ti	Si	Wt. Change Mg/Cm^2	Total N_2 Contamination (Wt%) 0 hr	100 hr	200 hr
Cr-6MgO(s)	110-1	18.1	9.6	15.5	+4.84	0.007		
	110-3	16.9	9.6	17.0	+4.56			0.0115
Cr-6MgO(e)	112-K	32.0	14.0	10.4	+2.02	0.008		
	112-L	31.0	14.3	11.5	+2.86			0.008

(l) = light

(h) = heavy

(s) = slurry sinter deposited barrier

(e) = electrophoretically deposited barrier layer

TABLE XVI - COMPOSITION OF SURFACE OXIDATION PRODUCTS ON UNCOATED AND COATED Cr-7Mo-2Ta ALLOY

Coating System	Spec. No.	Surface Composition
Cr-7Mo-2Ta	-	Cr_2O_3
Cr-Ti-Si (light)	6	Cr_2O_3 - TiO_2
Cr-Ti-Si (heavy)	115-2	Cr_2O_3
Cr-Y-12MgO (s)	112-9	Cr_2O_3
Cr-Y-12MgO (e)	111-C	Cr_2O_3 - TiO_2
Cr-Y-6MgO (e)	111-E	Cr_2O_3 - TiO_2
Cr-6MgO (e)	112-J	Cr_2O_3 - TiO_2
Cr-12MgO (s)	110-2	Cr_2O_3

(s) indicates slurry-sinter deposition of barrier layer

(e) indicates electrophoretic deposition of barrier layer

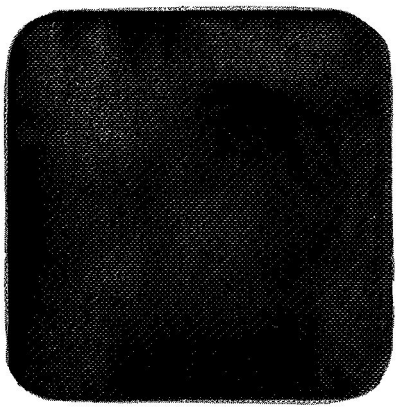

Figure 1. External View of Plasma Sprayed Iron-12MgO Coating.

(4X)

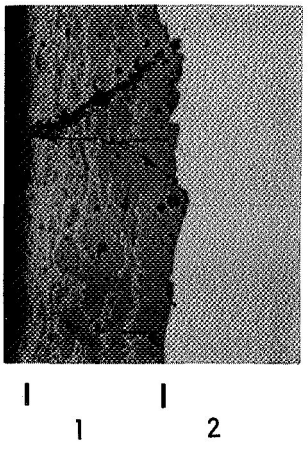

Figure 2. Photomicrograph of a Cross-Section Through a Plasma Sprayed Iron-12MgO Coating.

(250X Unetched)

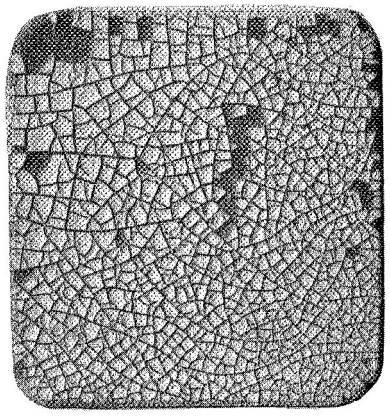

Figure 3. Plasma Sprayed Iron-12MgO Coating After 1 Hour in Hydrogen at 1800°F (1255°K)

(4X)

338 c

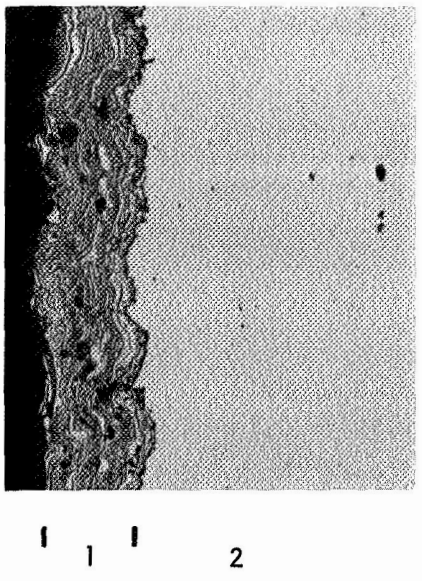

1 Coating
2 Substrate

Figure 4. Photomicrograph of a Cross-Section Through a Plasma Sprayed Chromium-MgO Coating.

(250X Unetched)

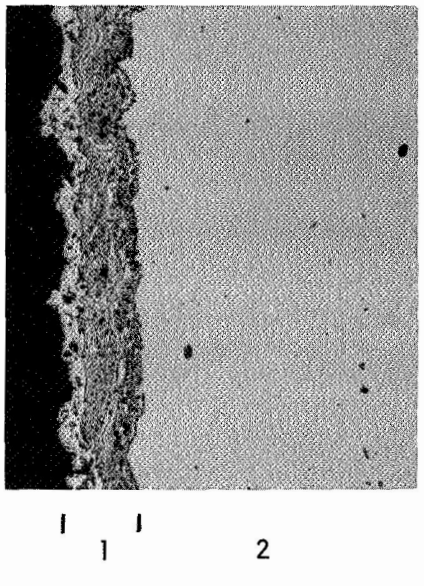

1 Coating
2 Substrate

Figure 5. Photomicrograph of a Cross-Section Through a Plasma Sprayed Chromium-MgO Coating After 1 Hour in Hydrogen at 2200°F (1477°K).

(250X Unetched)

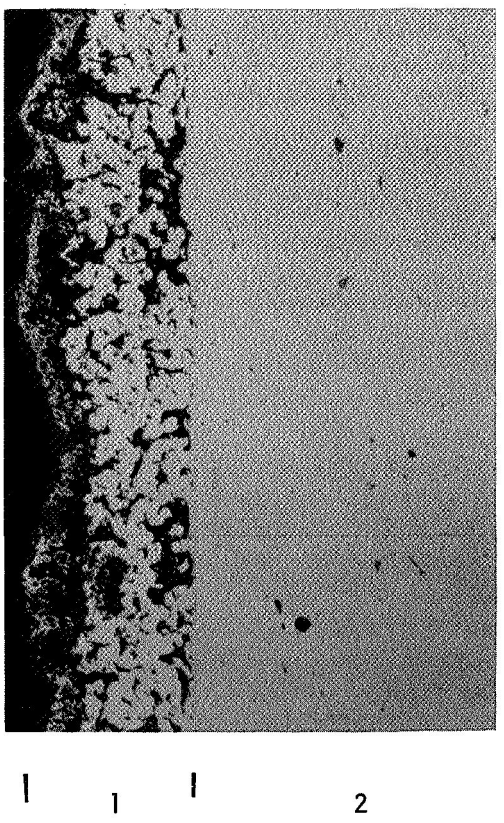

1 Coating
2 Substrate

Figure 6. Iron-12MgO Slurry-Sinter Coating on Cr-5W Alloy.
(250X Unetched)

340 c

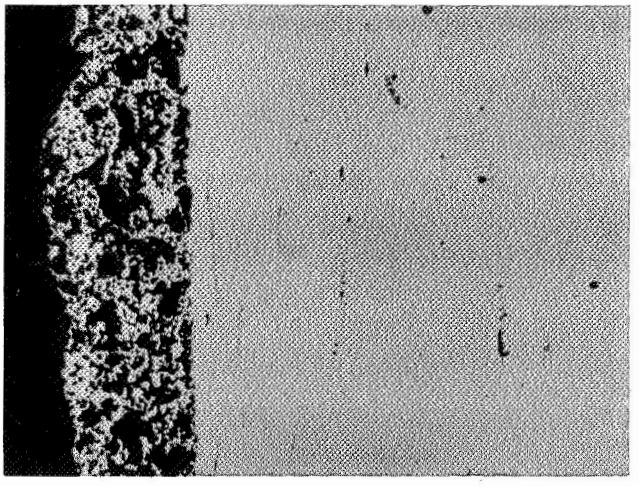

1 2

a) Light Microscopy (250X)

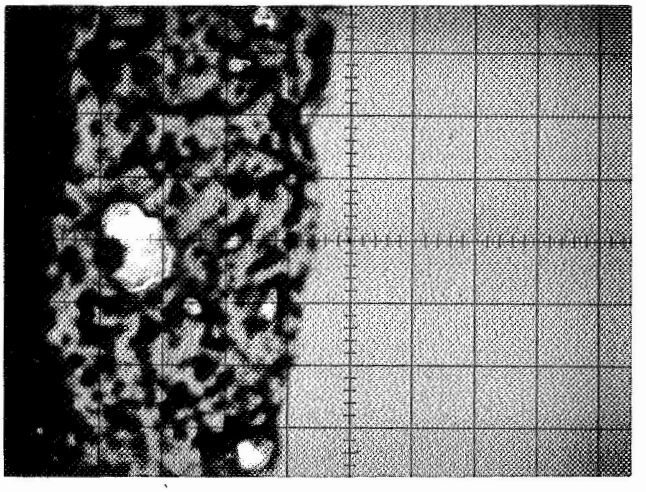

1 2

b) Electron Absorption (550X

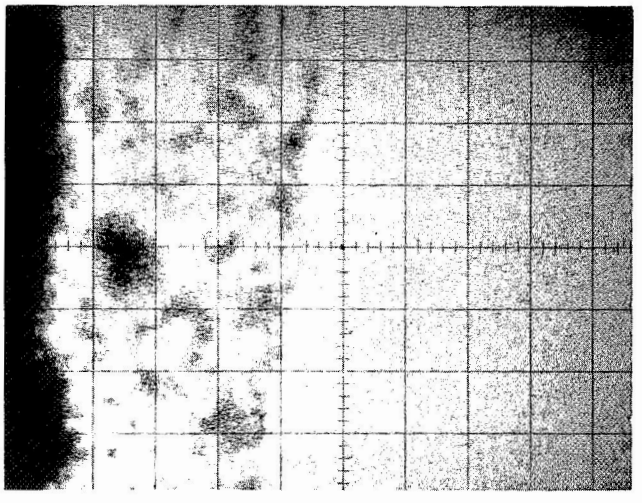

1 2

c) Cr X-rays (550X)

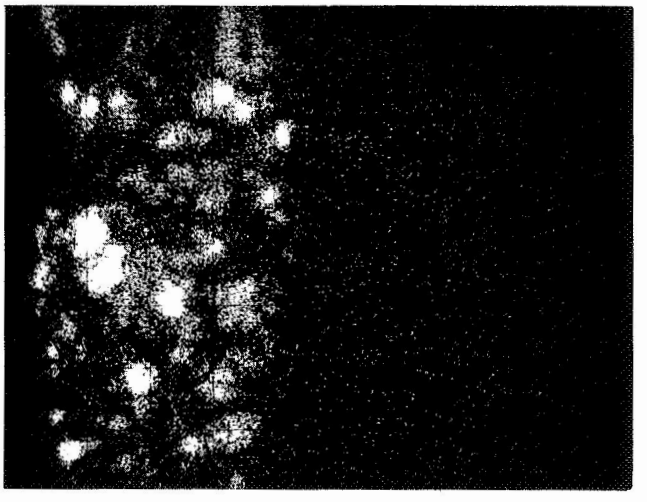

1 2

d) Mg X-rays (550X)

1 Barrier
2 Substrate

Figure 7. Slurry-Sinter Chromium-12MgO Coating on Cr-5W Alloy.

341 c

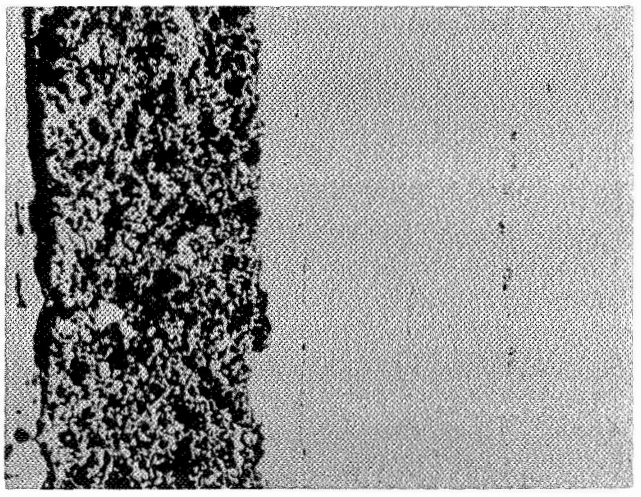

1 2

a) Light Microscopy (Etched)
(250X)

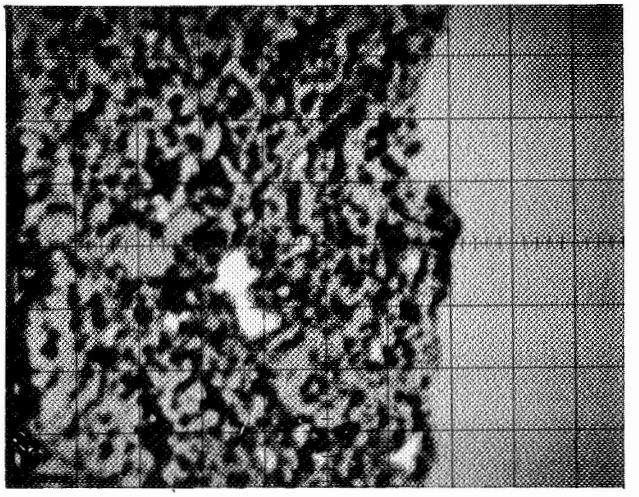

1 2

b) Electron Absorption
(550X)

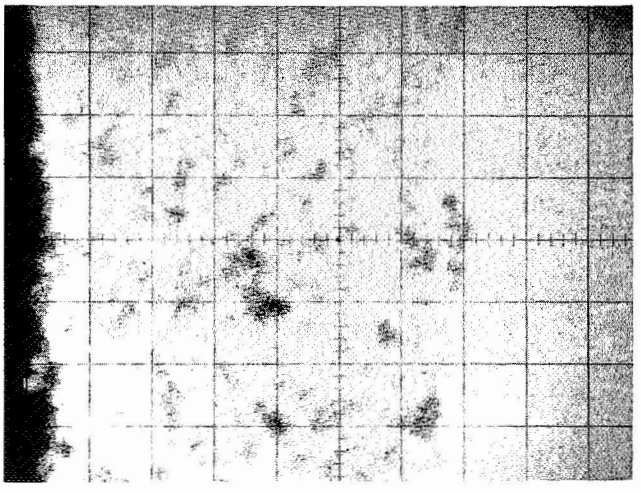

1 2

c) Cr X-rays
(550X)

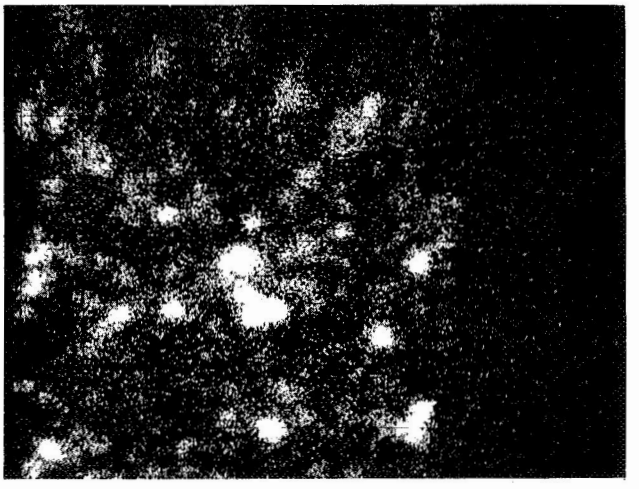

1 2

d) Mg X-rays
(550X)

1 Barrier Layer
2 Substrate

Figure 8. Distribution of MgO Particles in Electrophoretically Deposited Chromium-MgO Barrier Layer.

342 C

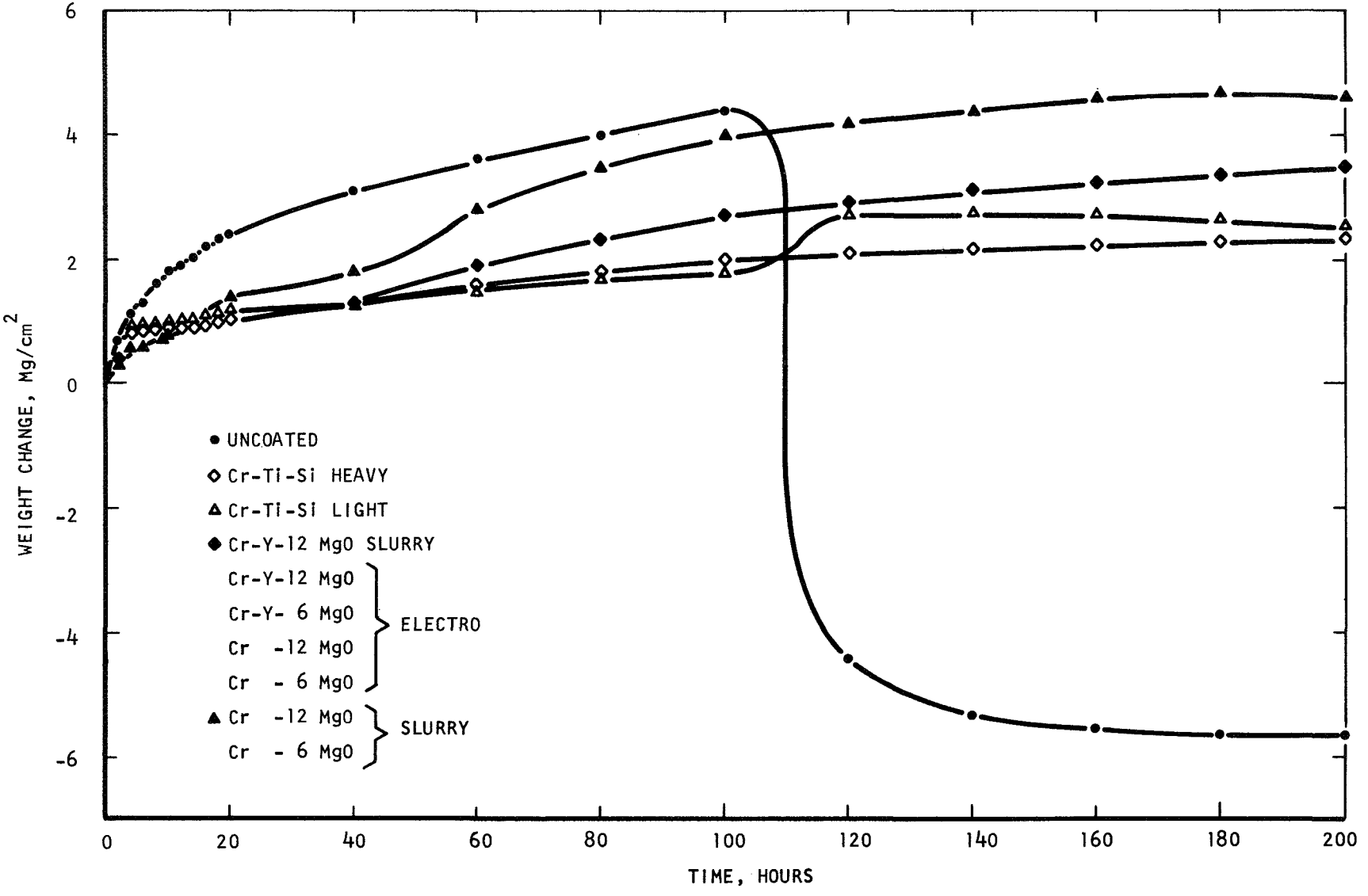

Figure 9. Oxidation Data for Coated and Uncoated Cr-7Mo-2Ta Alloy.

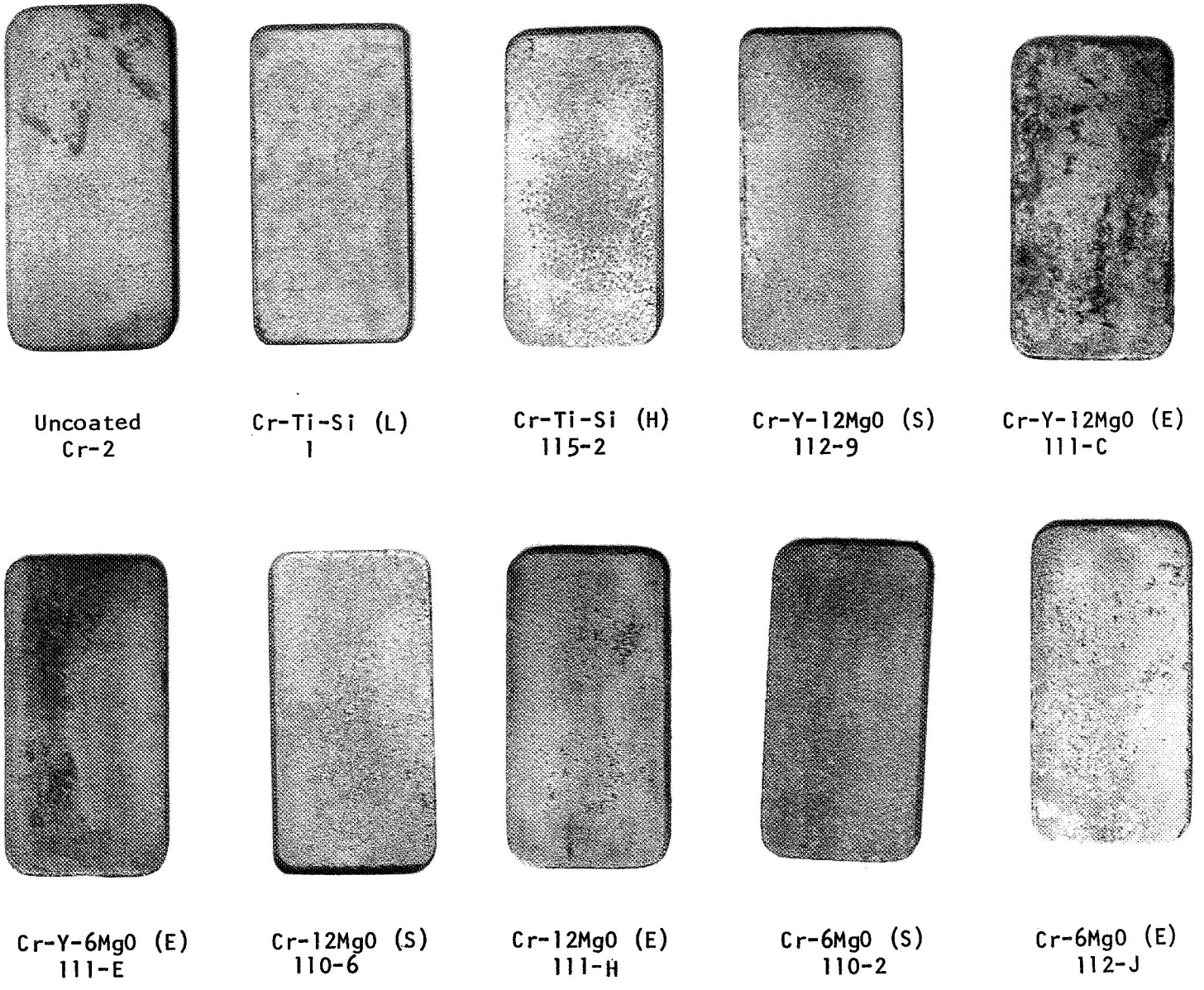

Figure 10. Photographs of Test Coupons After 200 Hours Exposure to 2100°F (1422°K) Air (Full Size).

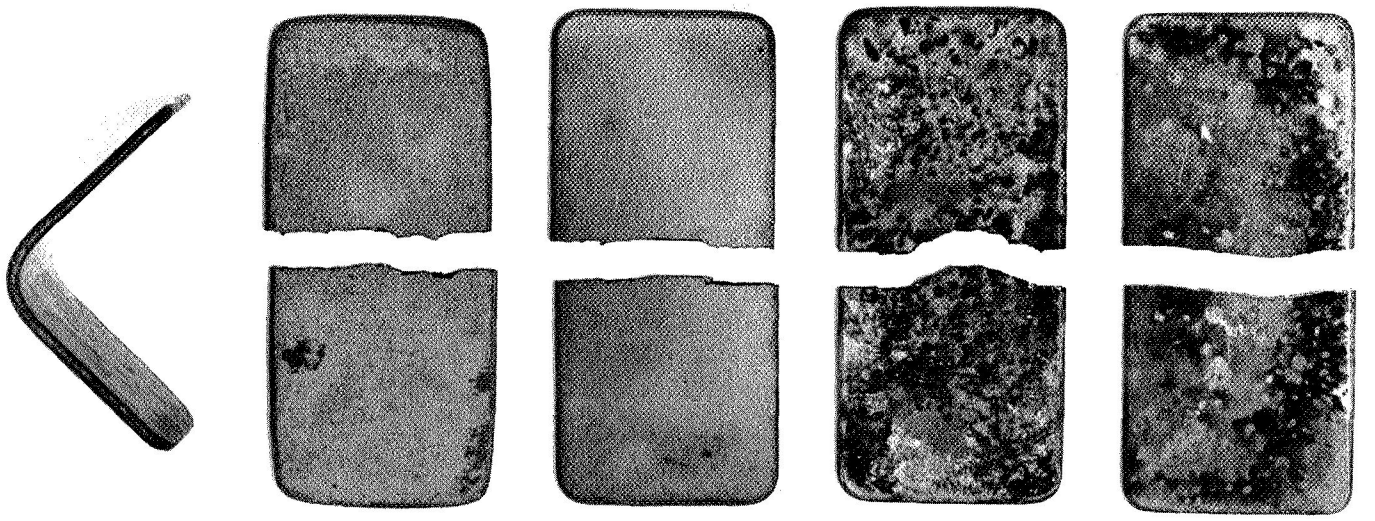

1 2 3 4 5

1. As-received coupon tested at 1090°F (861°K).
2. Cr-Ti-Si (light) coated, oxidized 100 hour at 2100°F (1420°K) and tested at 1490°F (1083°K).
3. Uncoated coupon given Cr-Ti-Si (light) thermal treatment and tested at 1490°F (1083°K).
4. Cr-Ti-Si (light) as-coated coupon tested at 1490°F (1083°K).
5. Cr-Ti-Si (light) as-coated coupon tested at 1090°F (861°K).

Figure 11. Post-Test Appearance of Typical DBTT Bend Test Evaluation Coupons. (1.25 X)

5656 B

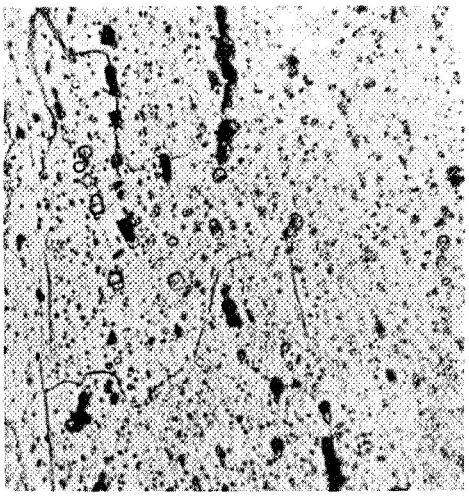

a) Light Microscopy (Etched)

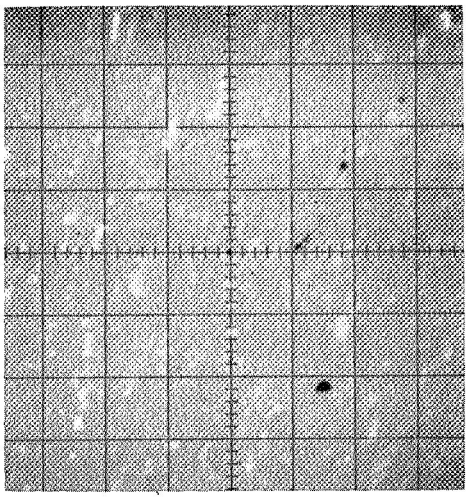

b) Electron Absorption

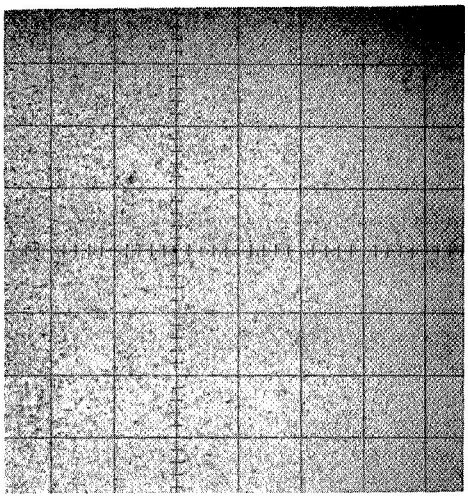

c) Cr X-rays

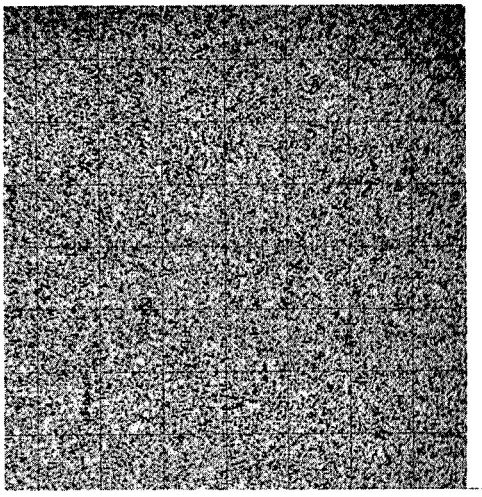

d) Mo X-rays

Figure 12. Photomicrograph and EMP Images of As-Received Cr-7Mo-2Ta Alloy.

(550X)

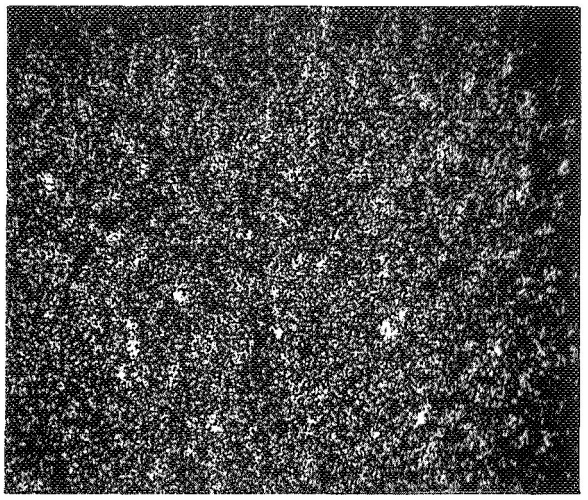

e) Ta X-rays

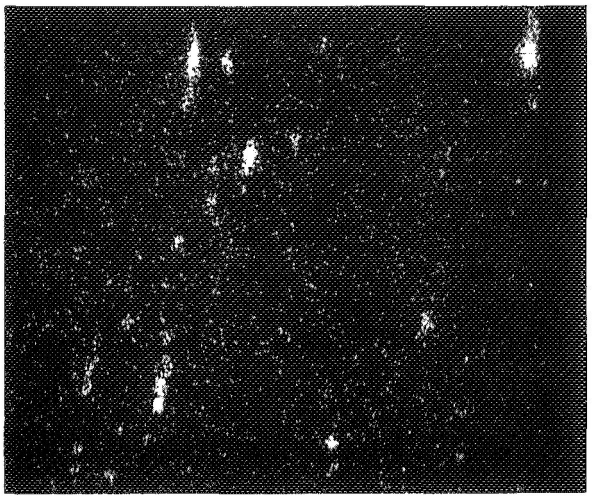

f) Y X-rays

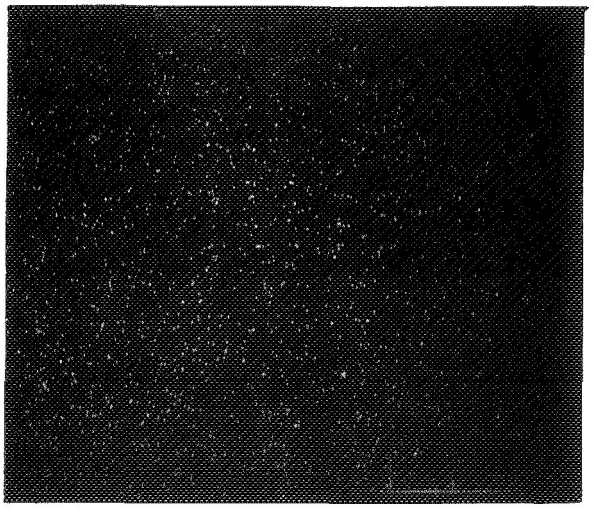

g) N X-rays

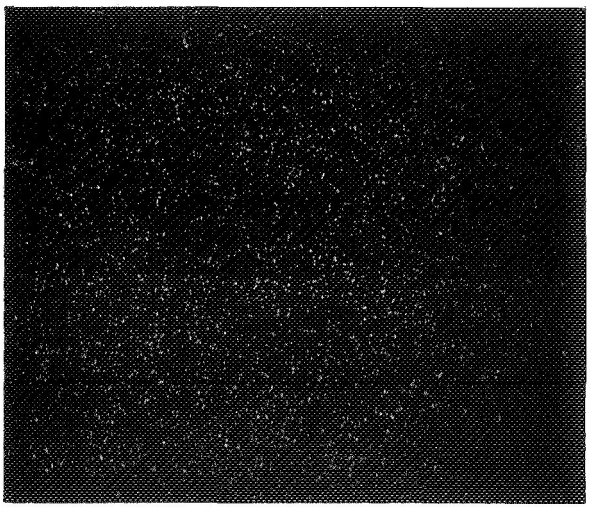

h) O X-rays

Figure 12 (Continued). Photomicrograph and EMP Images of As-Received Cr-7Mo-2Ta Alloy.

5643 B

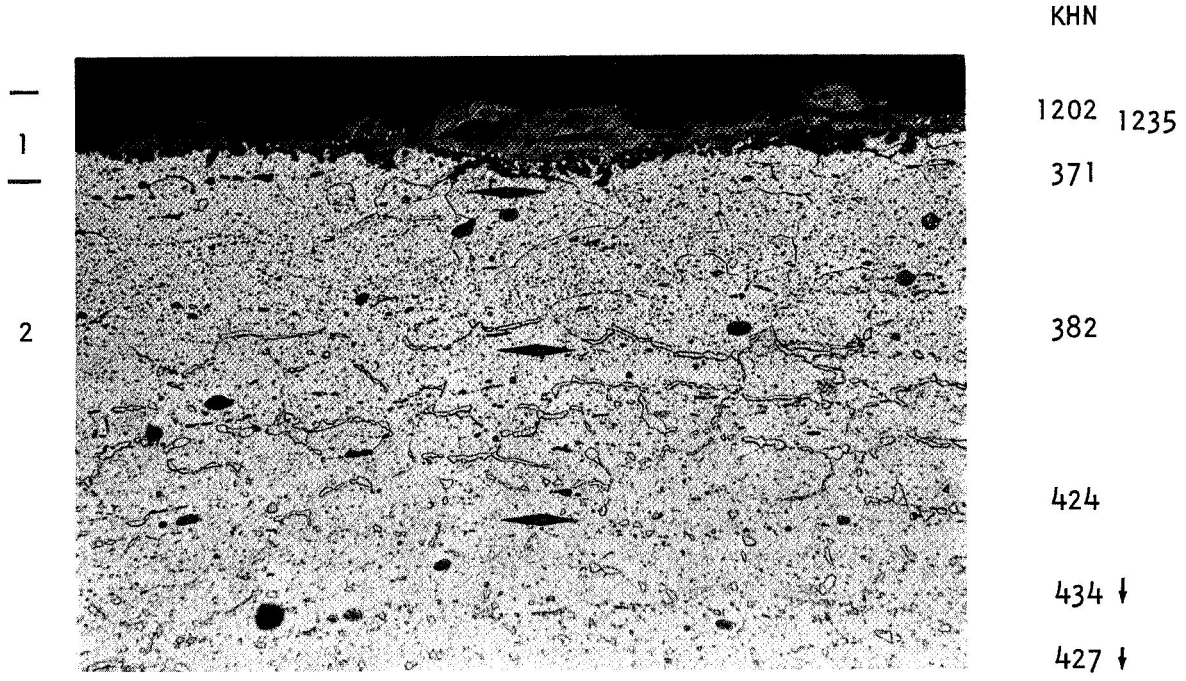

Figure 13. Photomicrograph and KHN Data for Cr-7Mo-2Ta After 200 Hours Exposure to Air at 2100°F (1422°K)

(250X Etched)

1 Coating

2 Substrate

5653 B

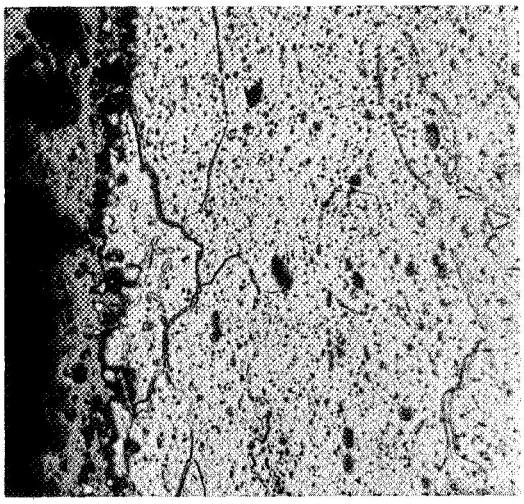

1 2

a) Light Microscopy (Etched)

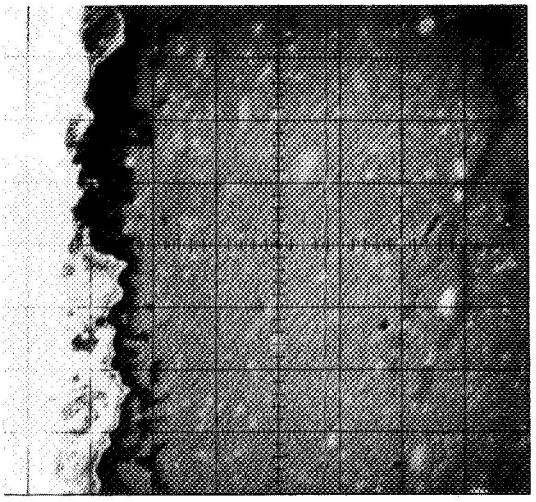

1 2

b) Electron Absorption

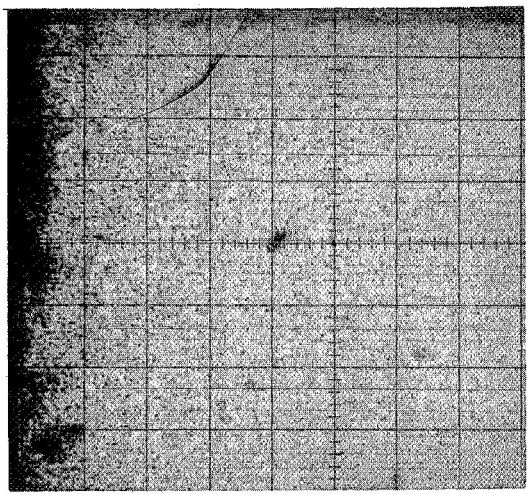

1 2

c) Cr X-rays

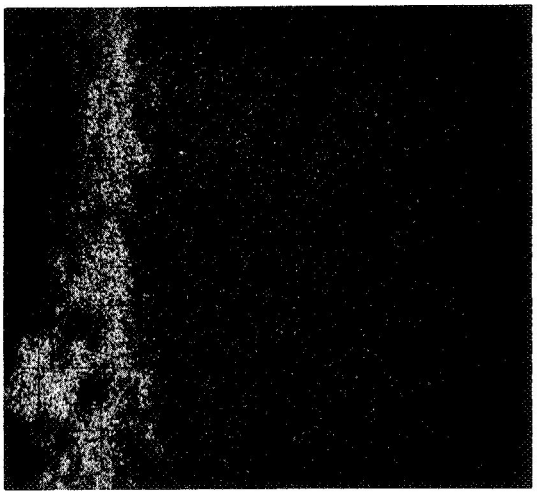

1 2

d) O X-rays

1 Oxide
2 Substrate

Figure 14. Photomicrograph and EMP Images of Cr-7Mo-2Ta After 200 Hours Oxidation at 2100°F (1422°K).

(550X)

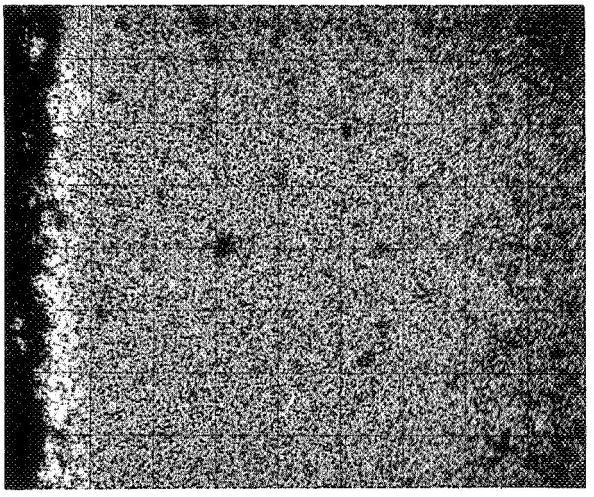

1 2

e) Mo X-rays

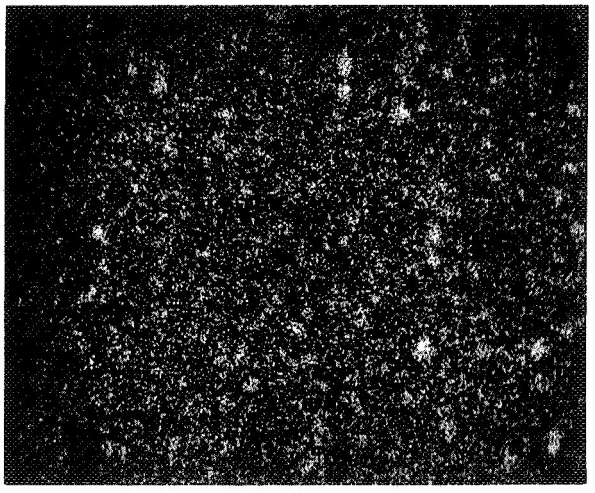

1 2

f) Ta X-rays

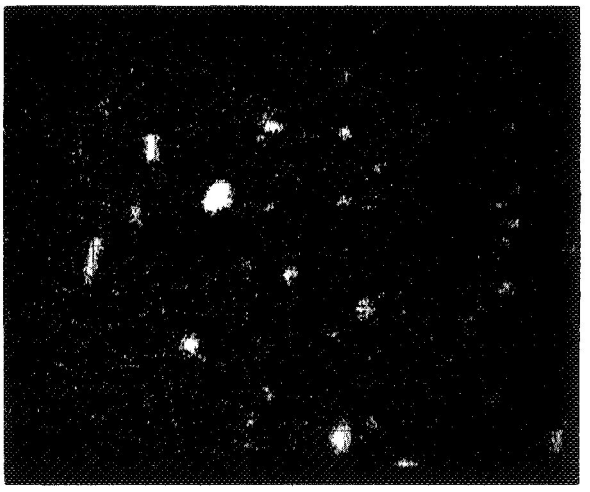

1 2

g) Y X-rays

1 Oxide
2 Substrate

Figure 14 (Continued). Photomicrograph and EMP Images of Cr-7Mo-2Ta After 200 Hours Oxidation at 2100°F (1422°K). (550X)

346 C

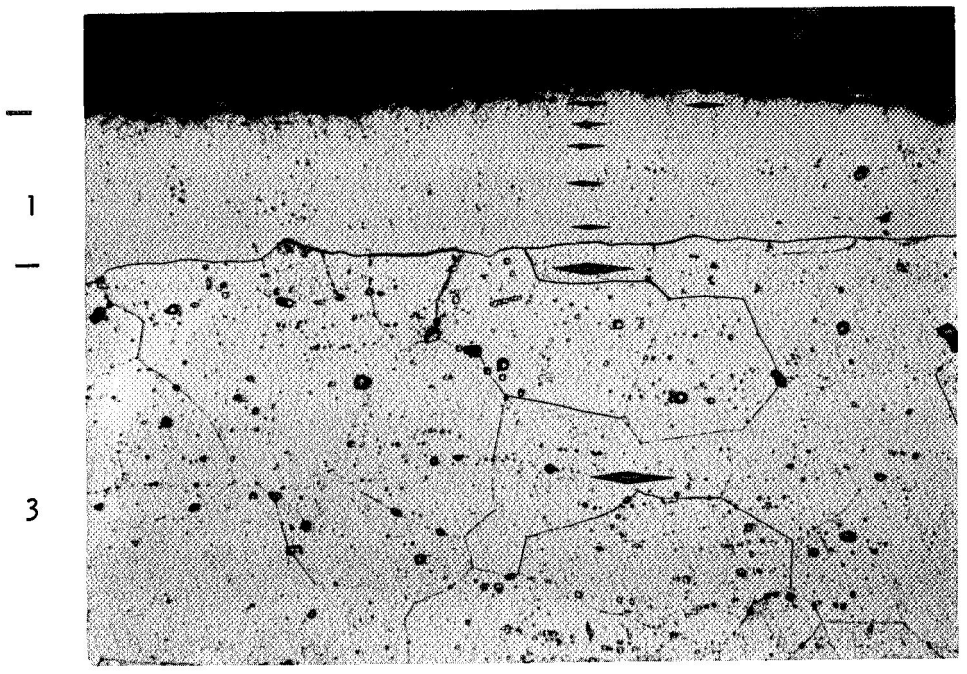

a) As-Coated

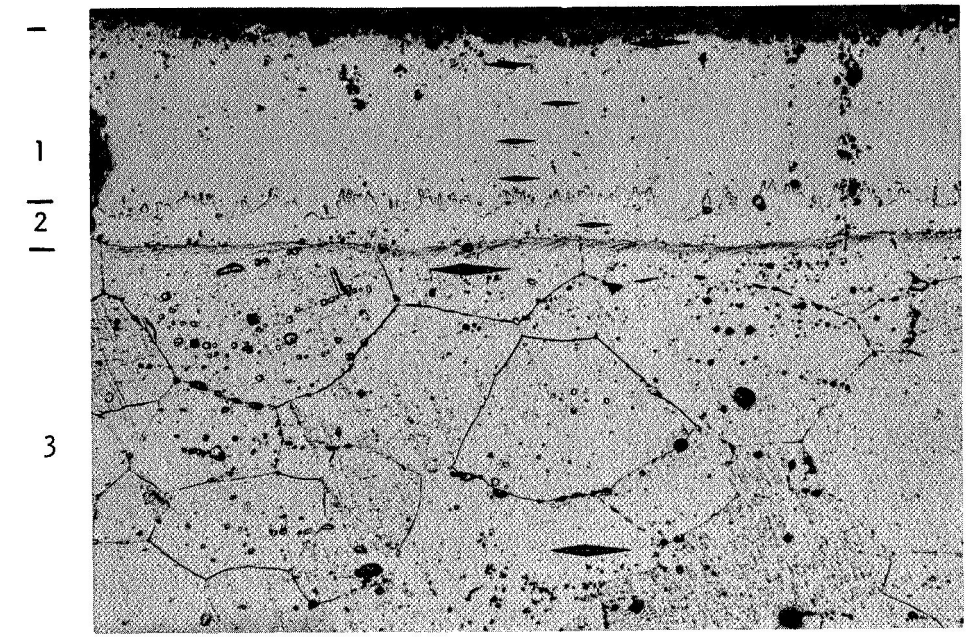

b) After 100 Hours Exposure

1 Coating
2 Diffusion Zone
3 Substrate

Figure 15. Microhardness Traverses in Cr-Ti-Si (Light) Coating. (250X Etched)

5661 B

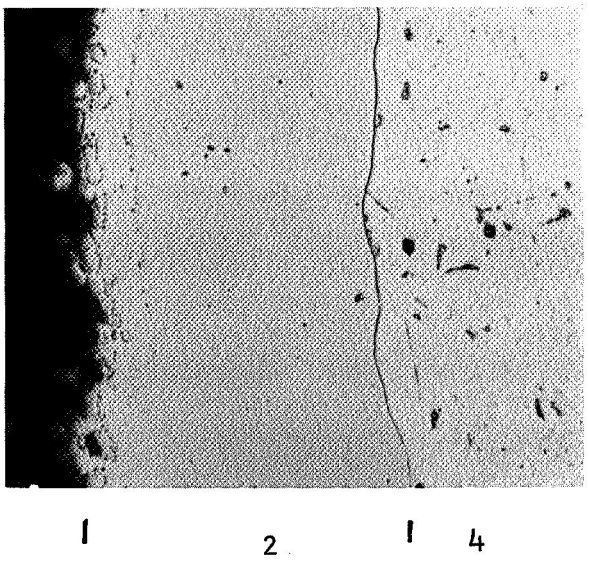

a) Light Microscopy (Etched)
As-Coated

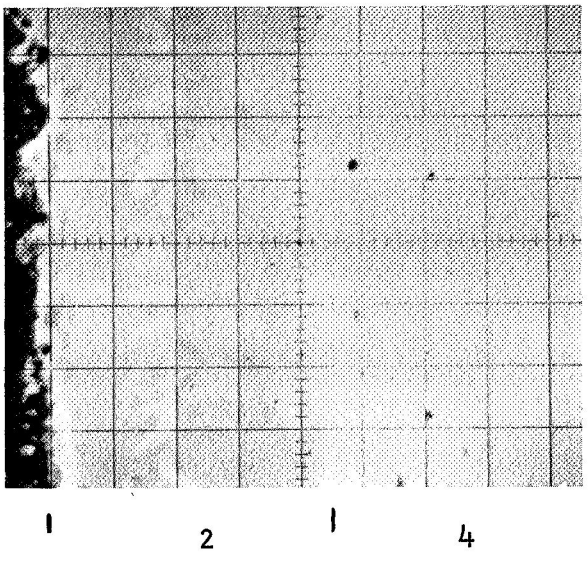

c) Electron Absorption
As-Coated

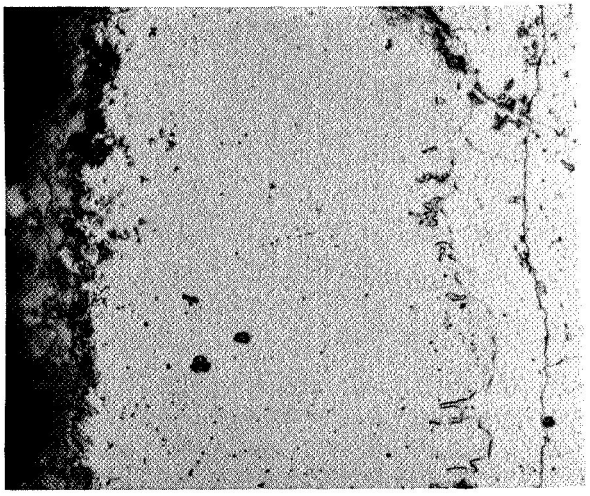

b) Light Microscopy (Etched)
After 100 Hours Exposure

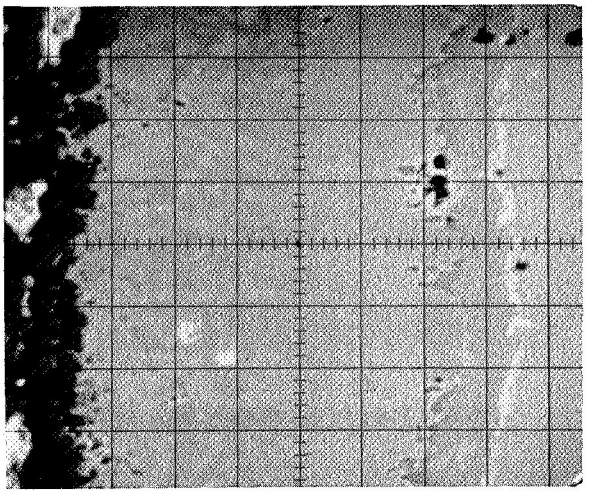

d) Electron Absorption
After 100 Hours Exposure

1 Oxide
2 Coating
3 Diffusion Zone
4 Substrate

Figure 16. Photomicrographs and EMP Images of the Cr-Ti-Si (Light) Coating As-Coated and After Exposure to 2100°F (1422°K).

(550X)

347 c

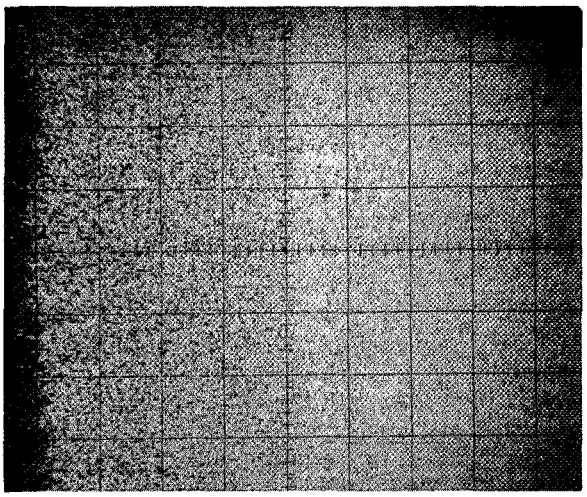

2 1 4

e) Cr X-rays
As-Coated

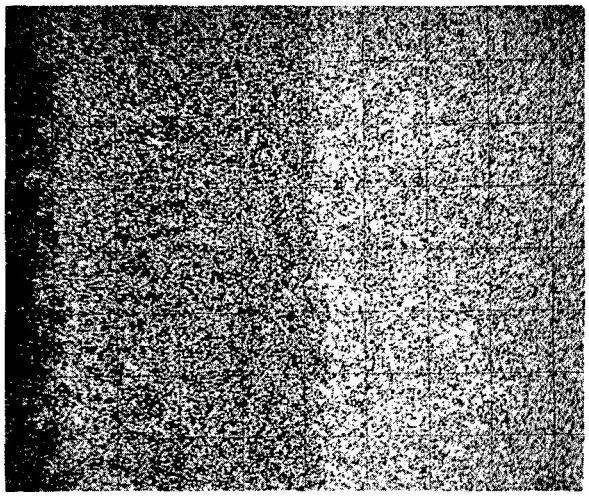

2 1 4

f) Mo X-rays
As-Coated

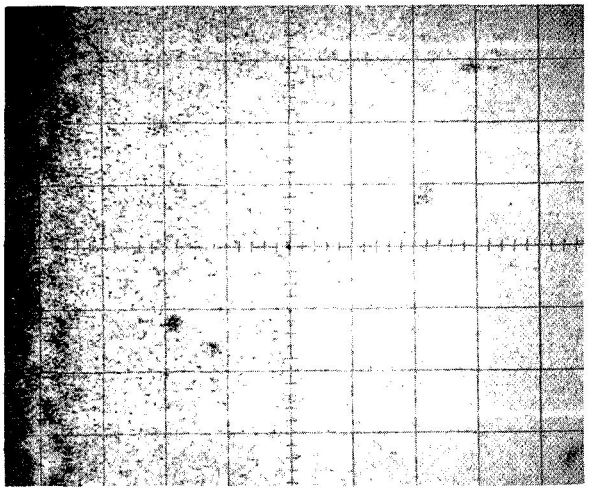

1 1 2 1 3 1 4

g) Cr X-rays
After 100 Hours Exposure

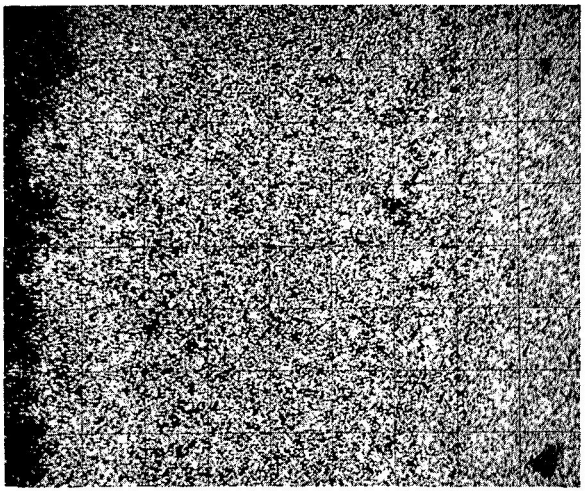

1 1 2 1 3 1 4

h) Mo X-rays
After 100 Hours Exposure

1 Oxide
2 Coating
3 Diffusion Zone
4 Substrate

Figure 16 (Continued). Photomicrographs and EMP Images of the Cr-Ti-Si (Light) Coating As-Coated and After Exposure to 2100°F (1422°K).

(550X)

348 c

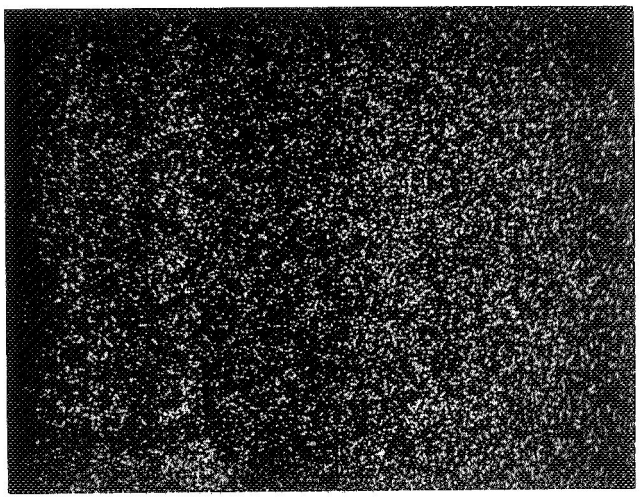

i) Ta X-rays
As-Coated

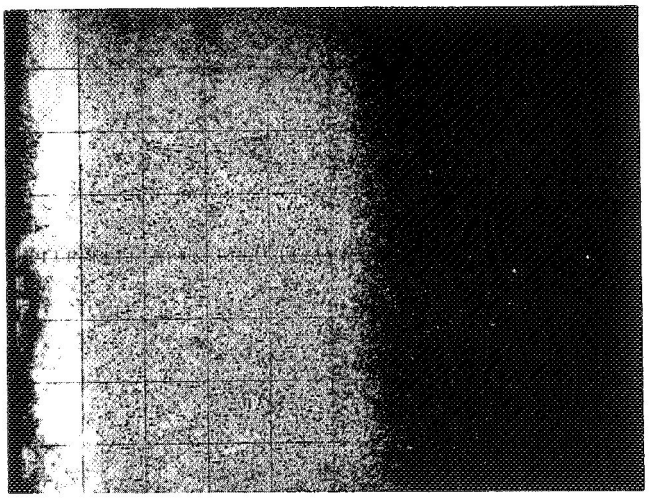

j) Ti X-rays
As-Coated

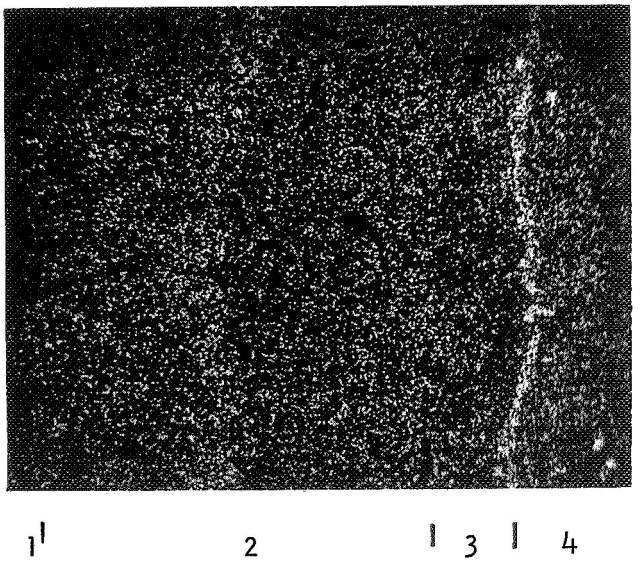

k) Ta X-rays
After 100 Hours Exposure

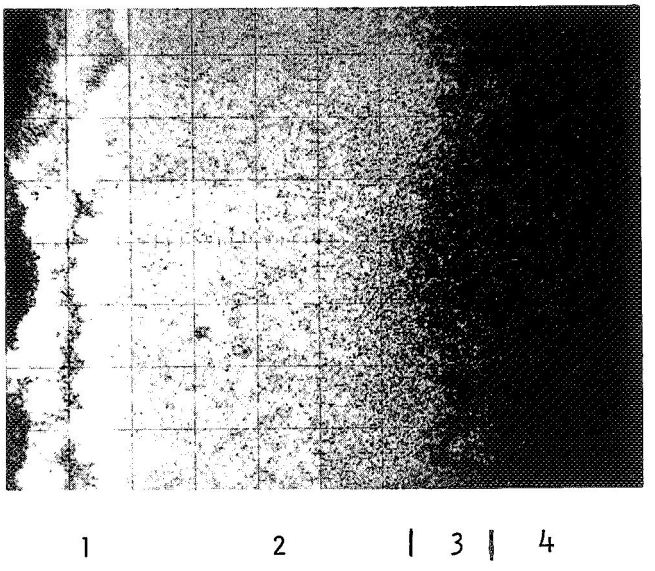

l) Ti X-rays
After 100 Hours Exposure

1 Oxide
2 Coating
3 Diffusion Zone
4 Substrate

Figure 16 (Continued). Photomicrographs and EMP Images of the Cr-Ti-Si (Light) Coating As-Coated and After Exposure to 2100°F (1422°K).
(550X)

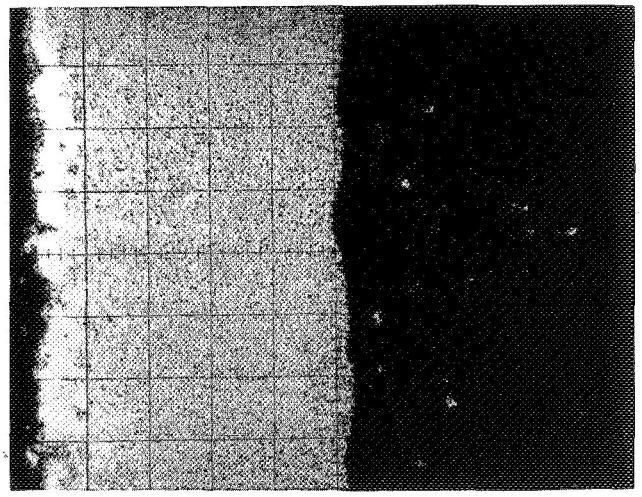

2 4

m) Si X-rays
As-Coated

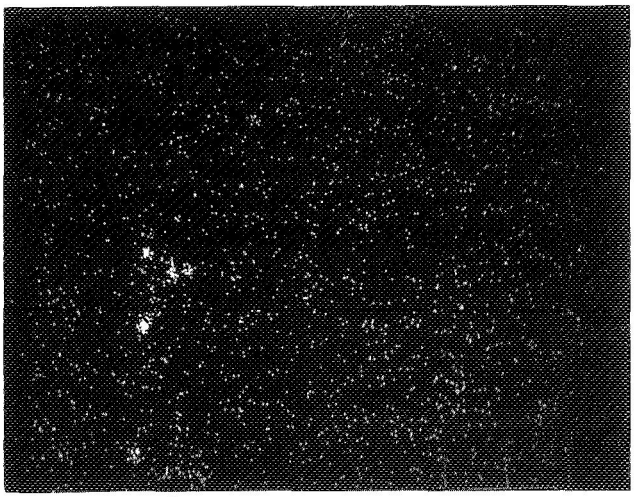

1 2 4

n) Y X-rays
As-Coated

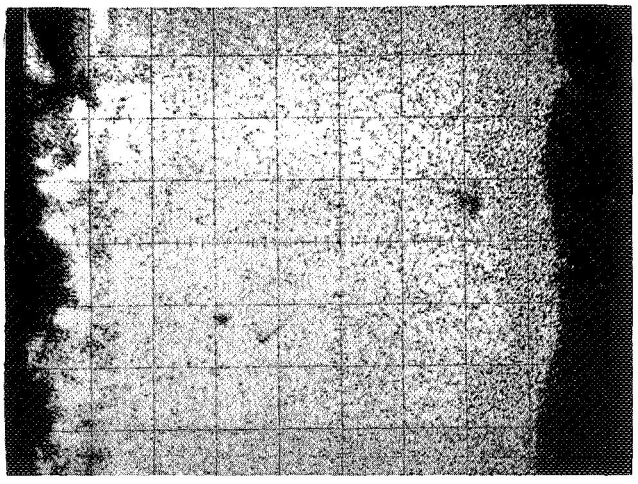

1 2 3 4

o) Si X-rays
After 100 Hours Exposure

1 2 3 4

p) Y X-rays
After 100 Hours Exposure

1 Oxide
2 Coating
3 Diffusion Zone
4 Substrate

Figure 16 (Continued). Photomicrographs and EMP Images of the Cr-Ti-Si (Light) Coating As-Coated and After Exposure to 2100°F (1422°K).

(550X)

350 c

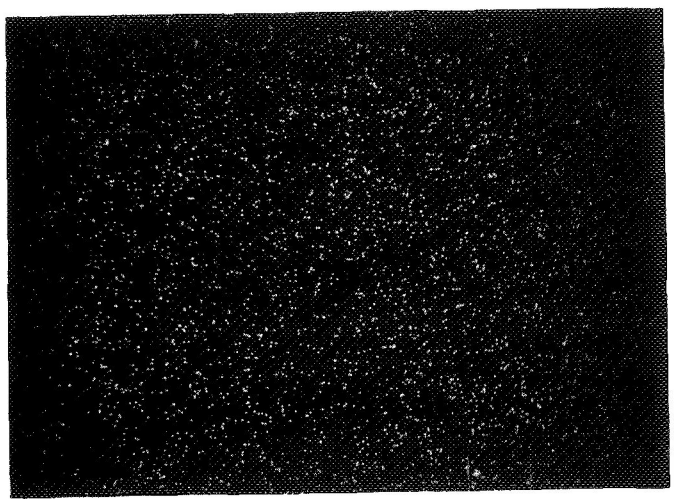

q) O_2 X-rays
As-Coated

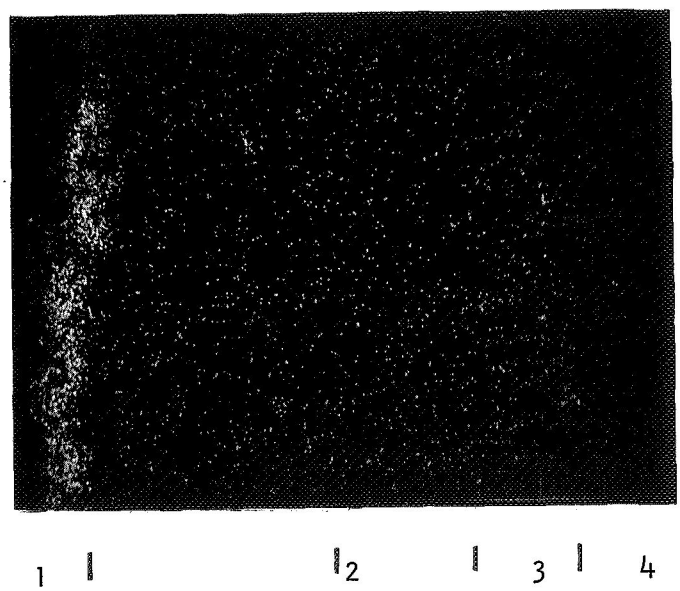

r) O_2 X-rays
After 100 Hours Exposure

1 Oxide
2 Coating
3 Diffusion Zone
4 Substrate

Figure 16 (Continued). Photomicrographs and EMP Images of the Cr-Ti-Si (Light) Coating As-Coated and After Exposure to 2100°F (1422°K).

(550X)

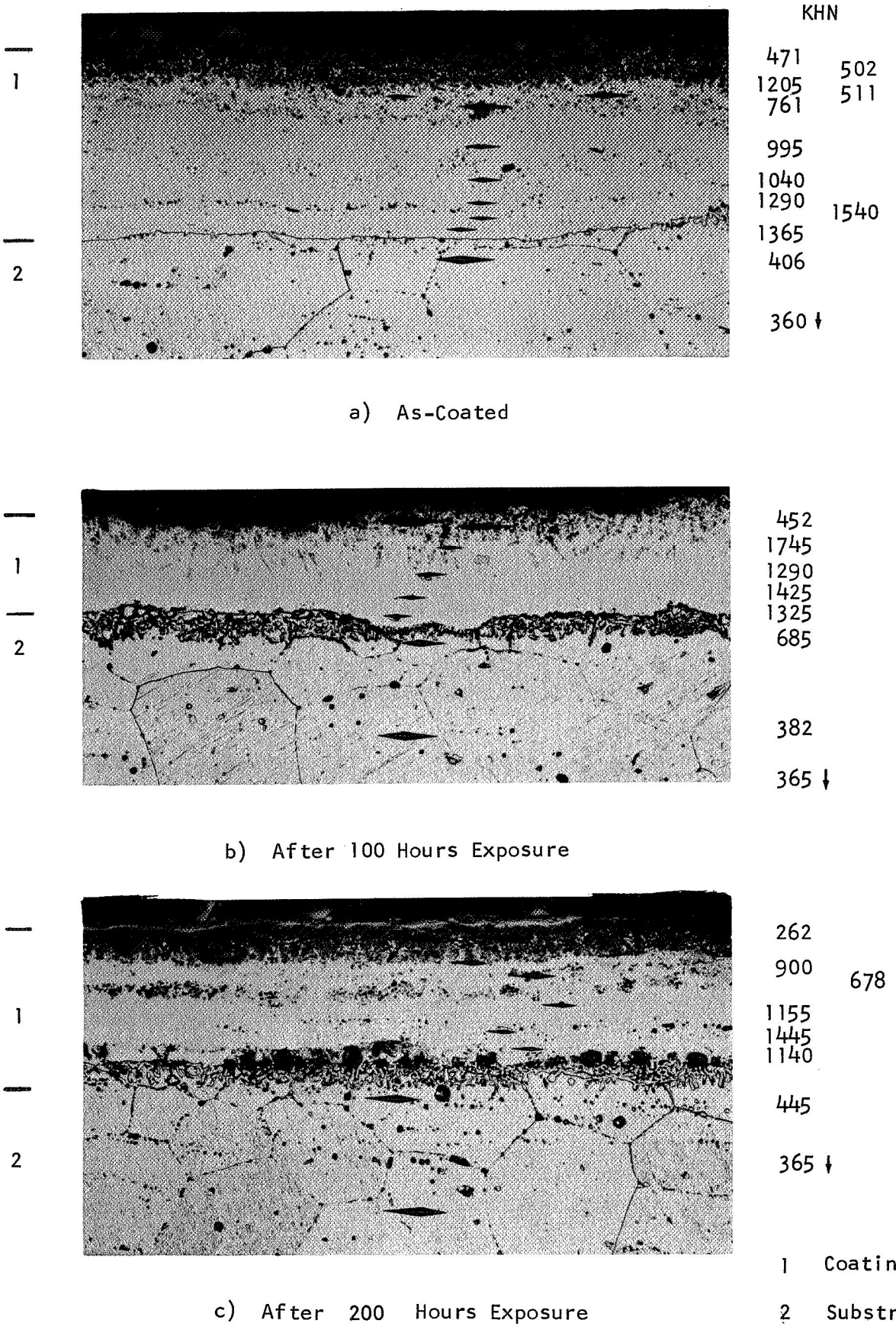

a) As-Coated

b) After 100 Hours Exposure

c) After 200 Hours Exposure

Figure 17. Microhardness Traverses in Cr-Ti-Si (Heavy) Coating. (250X Etched)

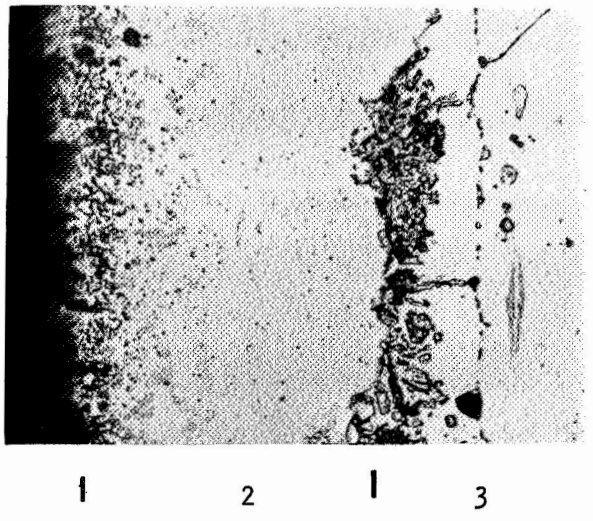

a) Light Microscopy (Etched)
As-Coated

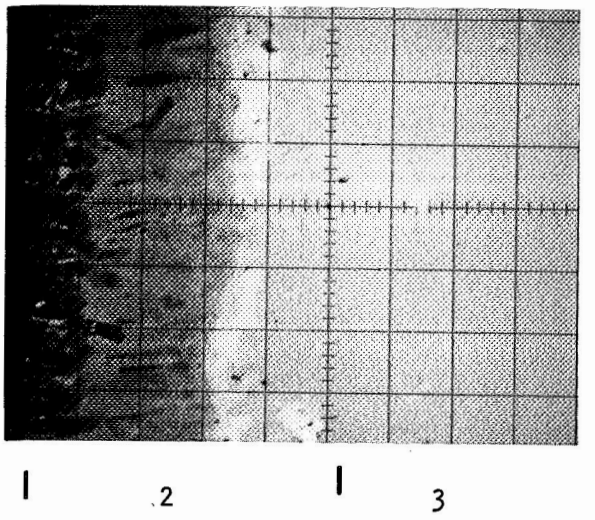

c) Electron Absorption
As-Coated

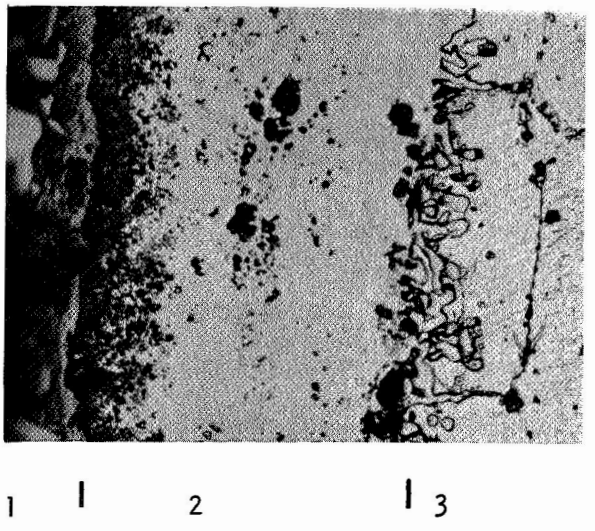

b) Light Microscopy (Etched)
After 200 Hours Exposure

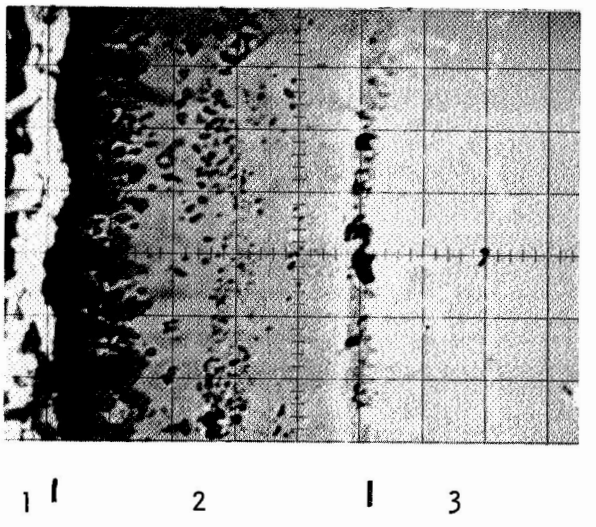

d) Electron Absorption
After 200 Hours Exposure

1 Oxide
2 Coating
3 Substrate

Figure 18. Photomicrographs and EMP Images of the Cr-Ti-Si (heavy) Coating System As-Coated and After 200 Hours Exposure to 2100°F (1422°K) Air. (550X)

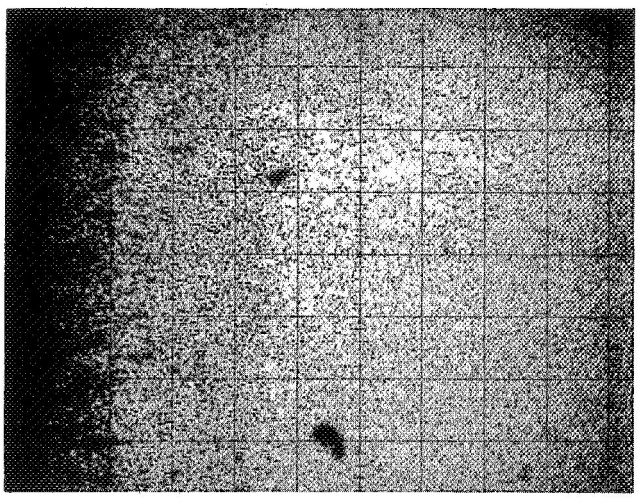

2 1 3

e) Cr X-rays
As-Coated

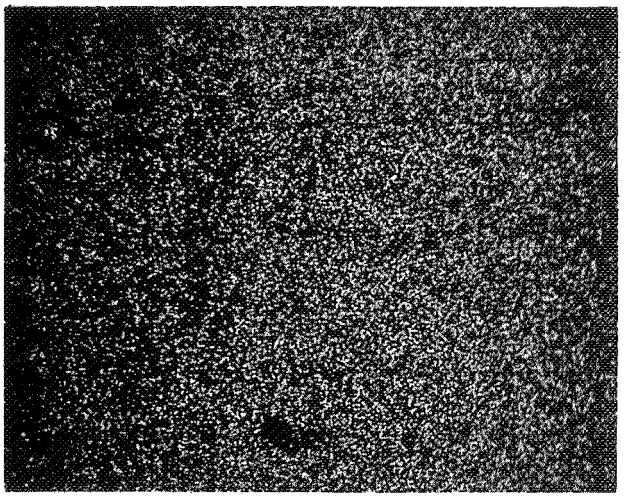

2 1 3

g) Mo X-rays
As-Coated

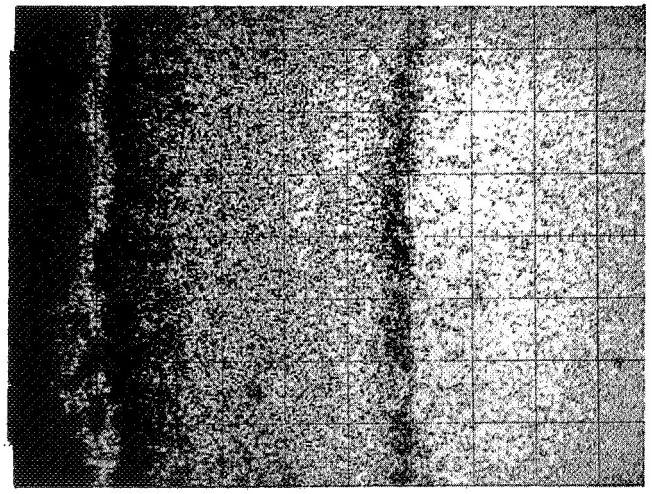

1 2 3

f) Cr X-rays
After 200 Hours Exposure

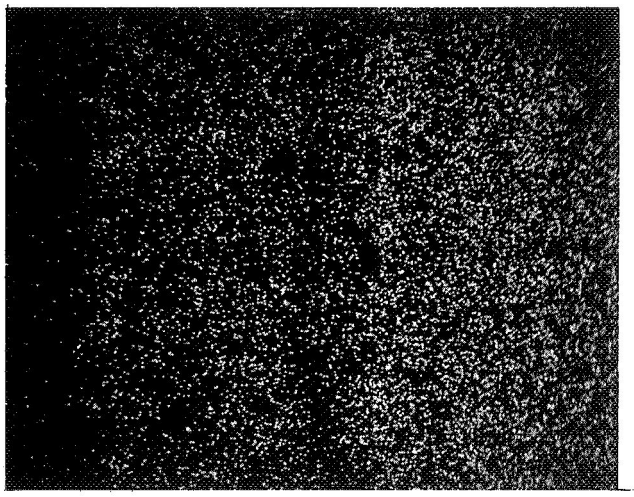

1 2 3

h) Mo X-rays
After 200 Hours Exposure

1 Oxide
2 Coating
3 Substrate

Figure 18 (Continued). Photomicrographs and EMP Images of the Cr-Ti-Si (heavy) Coating System As-Coated and After 200 Hours Exposure to 2100°F (1422°K) Air. (550X)

359 C

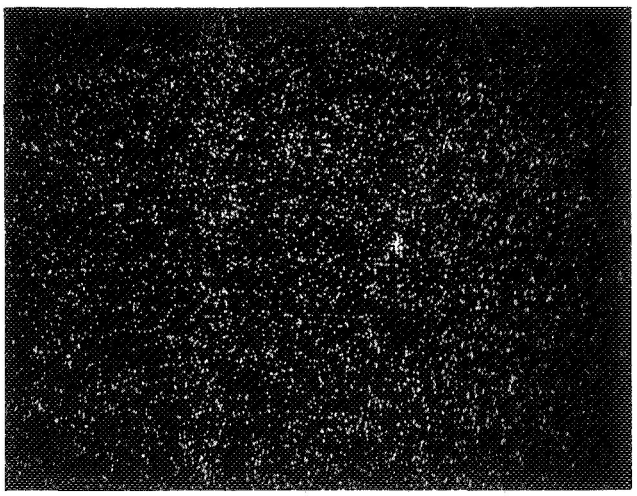

2 1 3

i) Ta X-rays
As-Coated

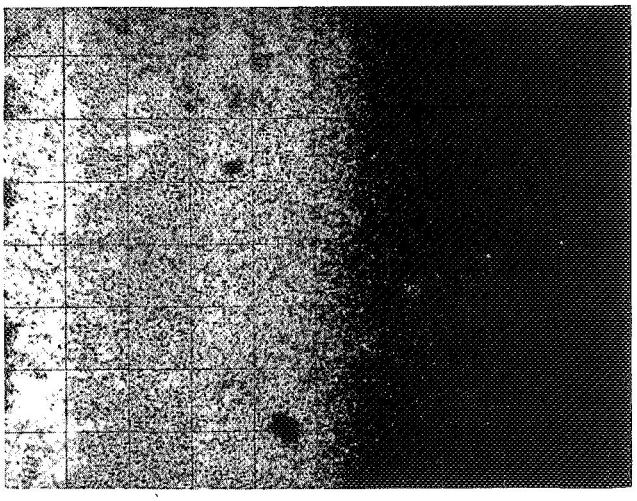

2 1 3

k) Ti X-rays
As-Coated

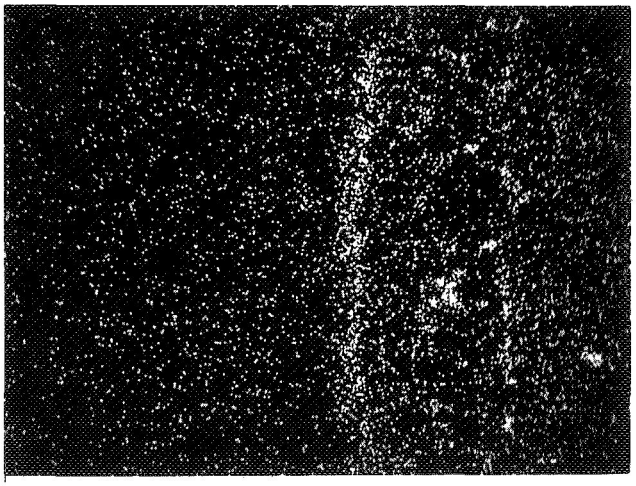

1 1 2 1 3

j) Ta X-rays
After 200 Hours Exposure

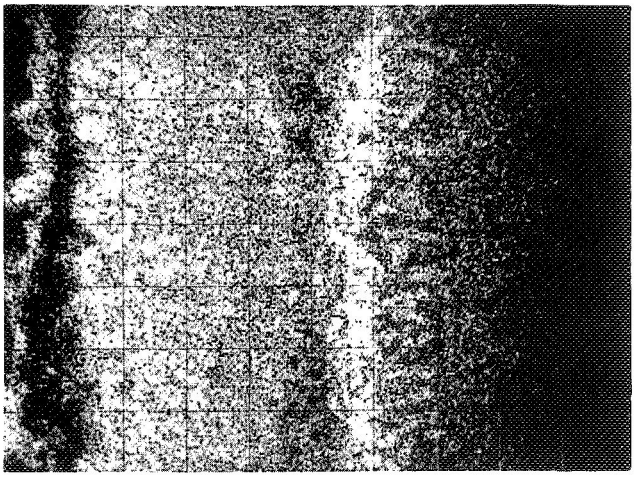

1 1 2 1 3

l) Ti X-rays
After 200 Hours Exposure

1 Oxide
2 Coating
3 Substrate

Figure 18 (Continued). Photomicrographs and EMP Images of the Cr-Ti-Si (heavy) Coating System As-Coated and After 200 Hours Exposure to 2100°F (1422°K) Air. (550X)

363 c

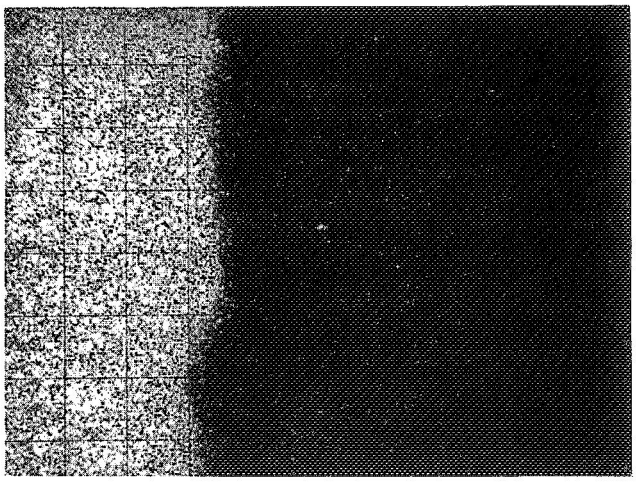

2 1 3

m) Si X-rays
As-Coated

2 1 3

o) Y X-rays
As-Coated

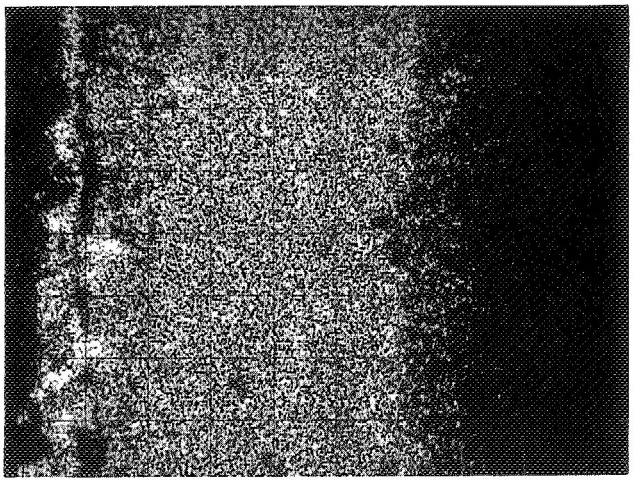

1 2 3

n) Si X-rays
After 200 Hours Exposure

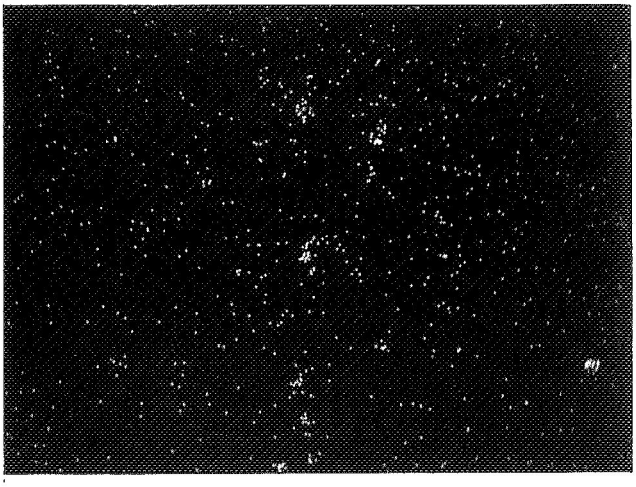

1 2 3

p) Y X-rays
After 200 Hours Exposure

1 Oxide
2 Coating
3 Substrate

Figure 18 (Continued). Photomicrographs and EMP Images of the Cr-Ti-Si (heavy) Coating System As-Coated and After 200 Hours Exposure to 2100°F (1422°K) Air. (550X)

364 c

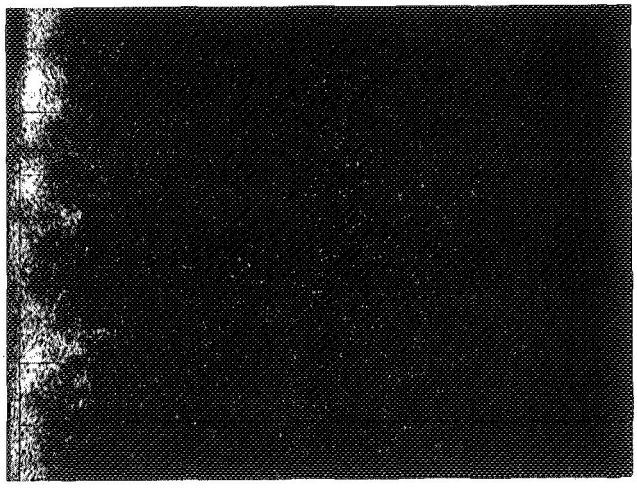

2 1 3

q) Al X-rays
As-Coated

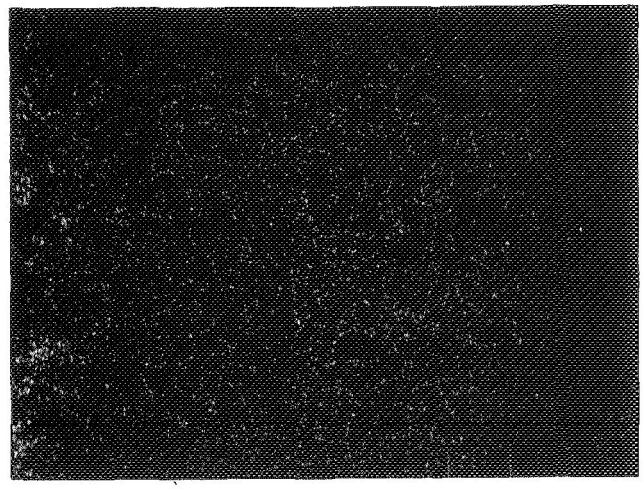

2 1 3

s) O X-rays
As-Coated

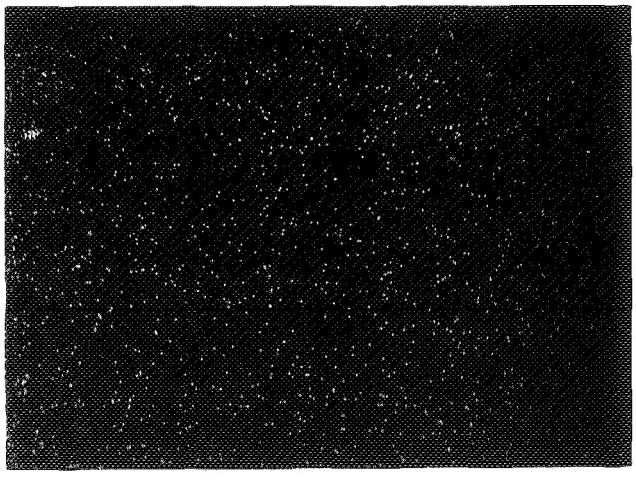

1 2 3

r) Al X-rays
After 200 Hours Exposure

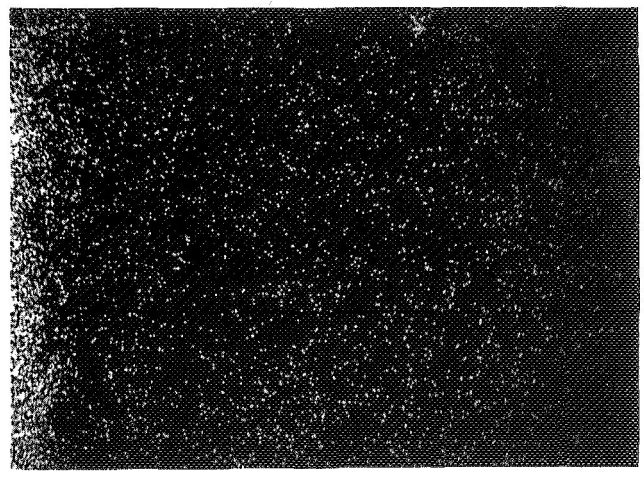

1 2 3

t) O X-rays
After 200 Hours Exposure

1 Oxide
2 Coating
3 Substrate

Figure 18 (Continued). Photomicrographs and EMP Images of the Cr-Ti-Si (heavy) Coating System As-Coated and After 200 Hours Exposure to 2100°F (1422°K) Air. (550X)

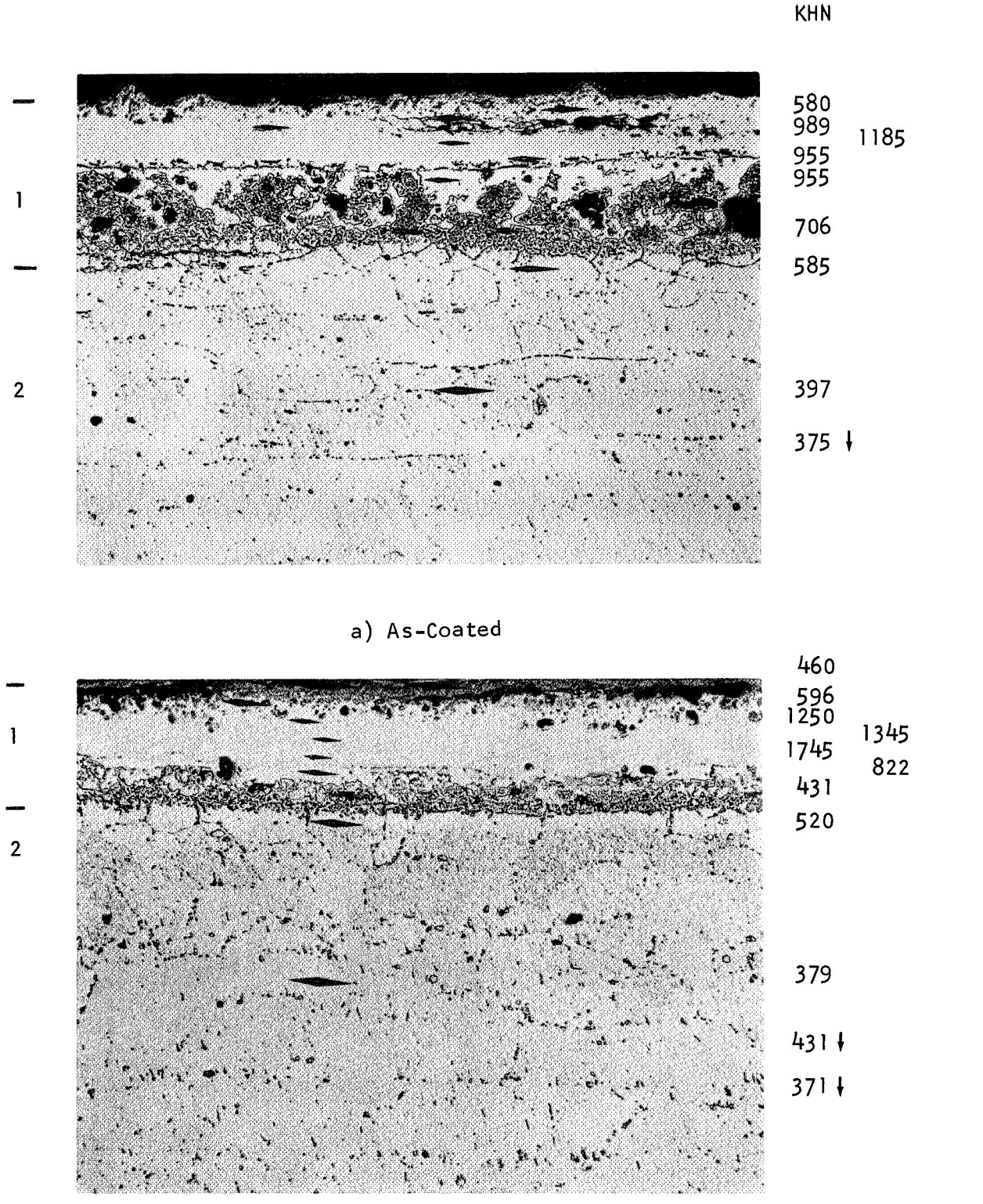

Figure 19. Microhardness Traverses in Cr-12MgO/Cr-Ti-Si Coating. (250X Etched)

5655 B

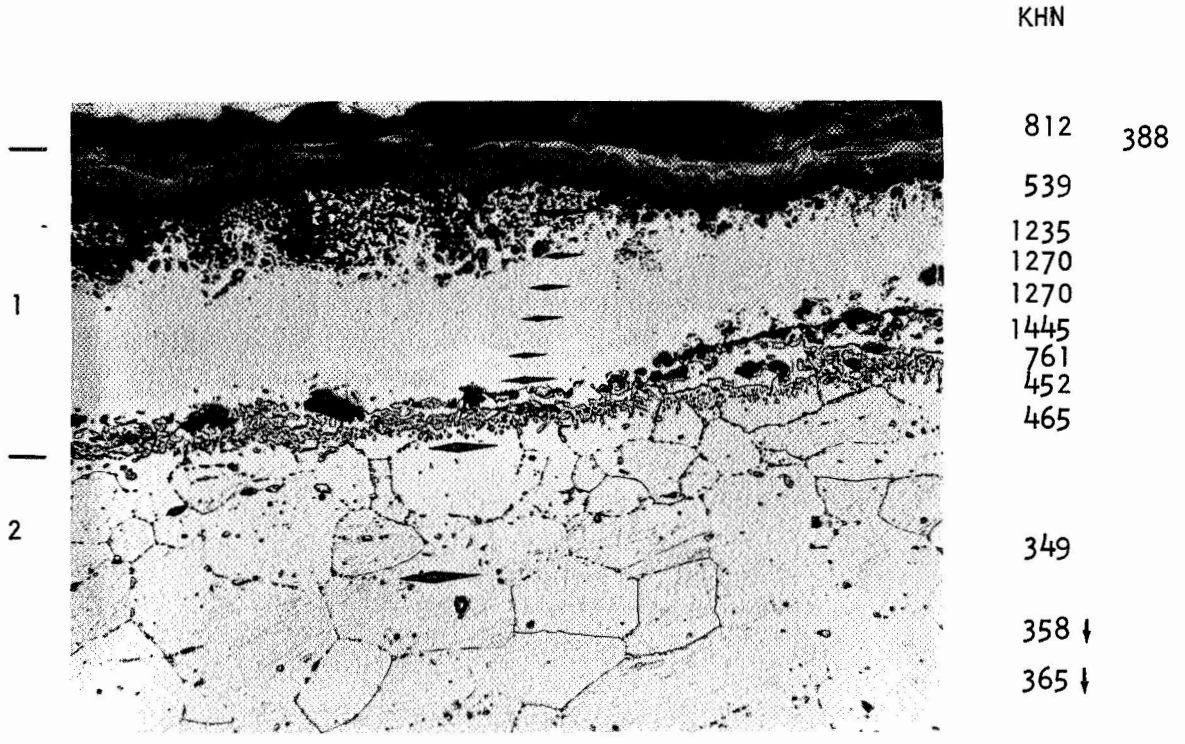

c) After 200 Hours Exposure

1 Coating

2 Substrate

Figure 19 (Continued). Microhardness Traverses in Cr-12MgO/Cr-Ti-Si Coating.

(250X Etched)

5654 B

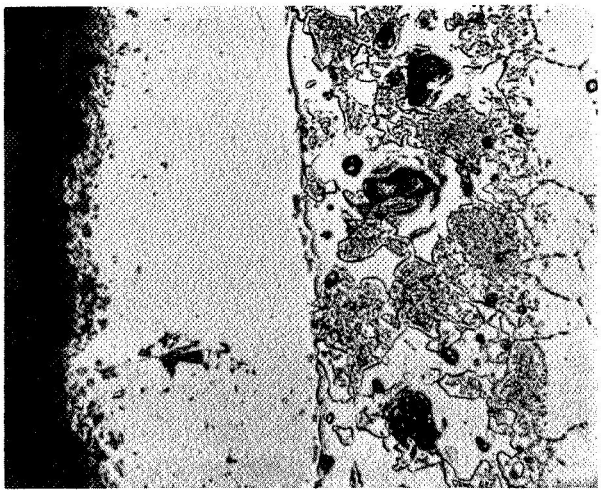

a) Light Microscopy (Etched)
As-Coated

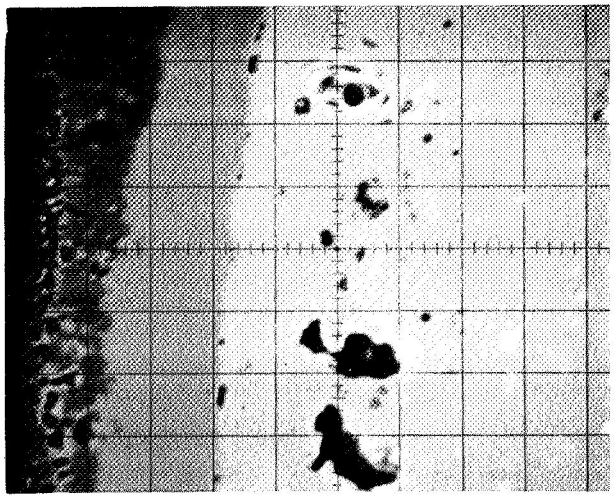

c) Electron Absorption
As-Coated

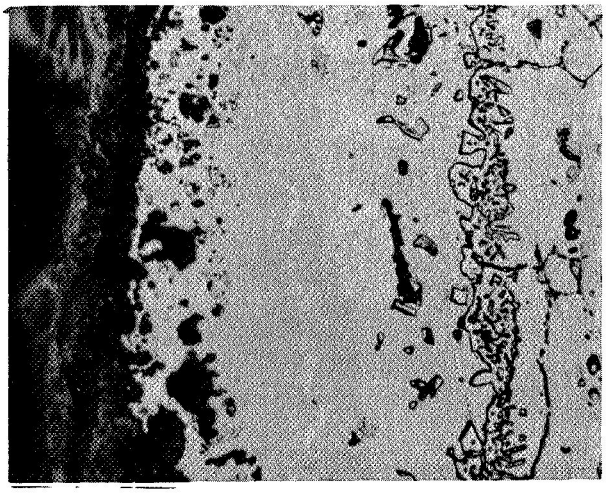

b) Light Microscopy (Etched)
After 200 Hours Exposure

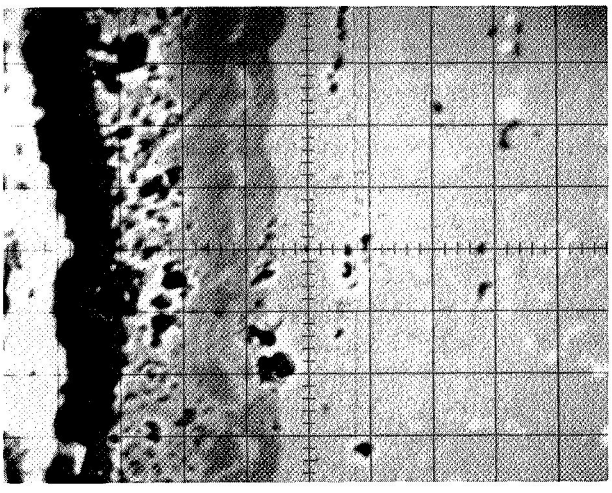

d) Electron Absorption
After 200 Hours Exposure

1 Oxide
2 Coating
3 Barrier
4 Substrate

Figure 20. Photomicrographs and EMP Images of the Cr-12MgO/Cr-Ti-Si Coating System As-Coated and After 200 Hours Exposure to 2100°F (1422°K) Air.

(550X)

367 c

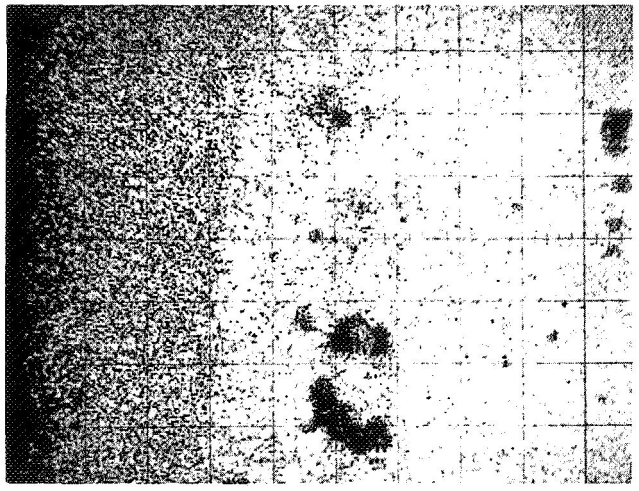

e) Cr X-rays
As-Coated

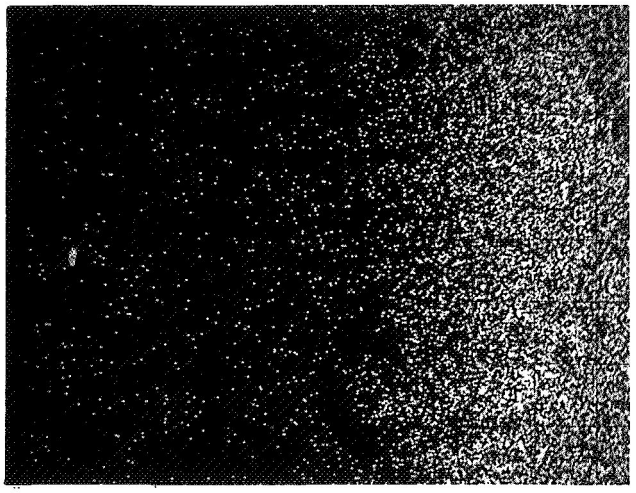

g) Mo X-rays
As-Coated

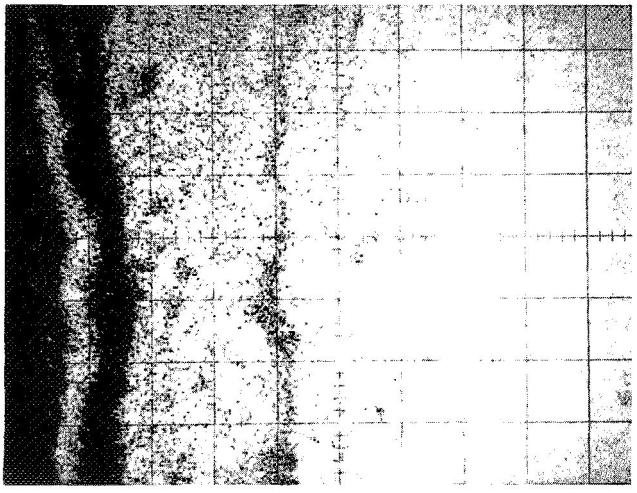

f) Cr X-rays
After 200 Hours Exposure

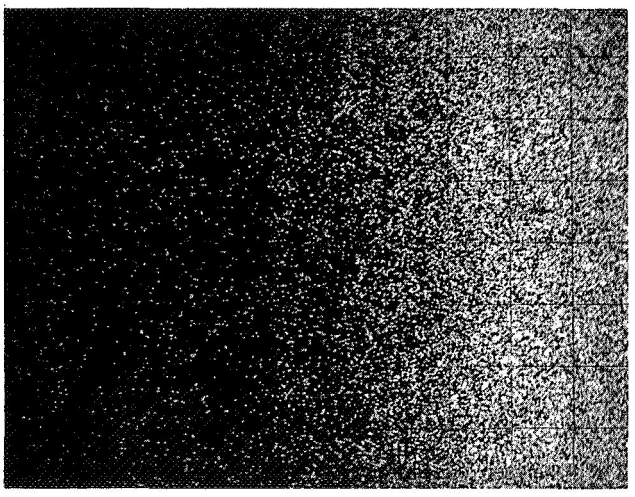

h) Mo X-rays
After 200 Hours Exposure

1 Oxide
2 Coating
3 Barrier
4 Substrate

Figure 20 (Continued). Photomicrographs and EMP Images of the Cr-12MgO/Cr-Ti-Si Coating System As-Coated and after 200 Hours Exposure to 2100°F (1422°K) Air.
(550X)

368 c

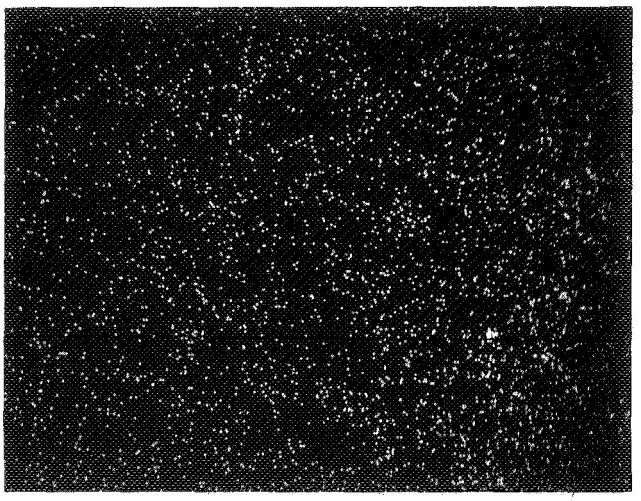

2 1 3 4

i) Ta X-rays
As-Coated

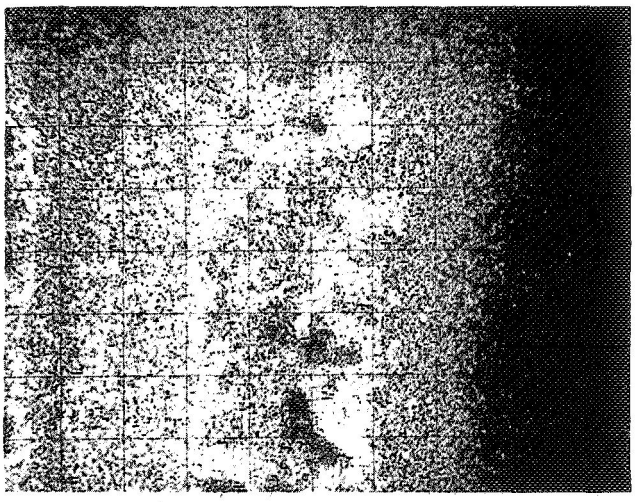

1 2 3

k) Ti X-rays
As-Coated

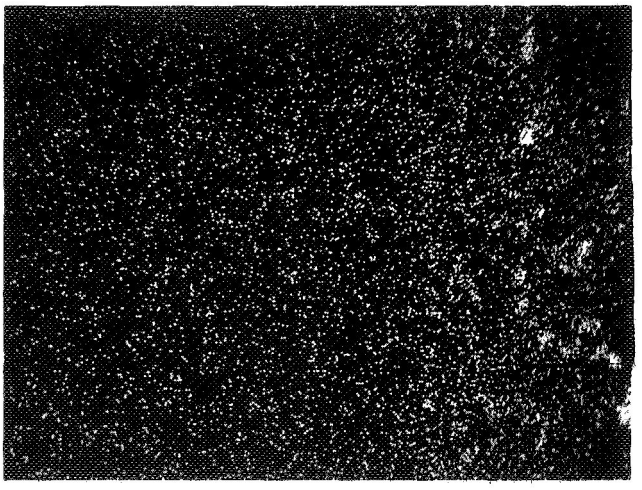

1 2 3 4

j) Ta X-rays
After 200 Hours Exposure

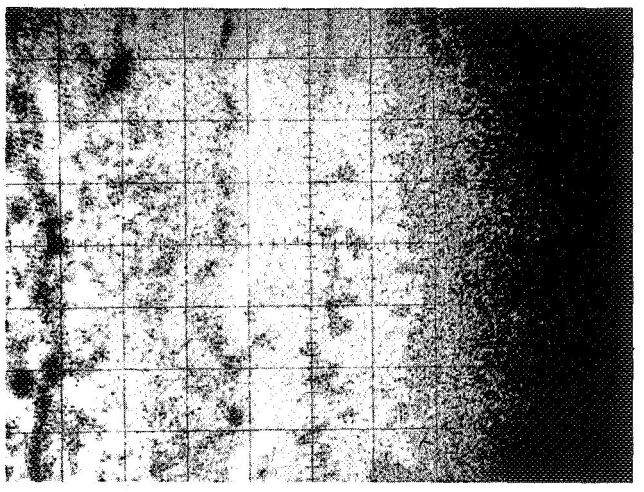

1 2 3 4

l) Ti X-rays
After 200 Hours Exposure

1 Oxide
2 Coating
3 Barrier
4 Substrate

Figure 20 (Continued). Photomicrographs and EMP Images of the Cr-12MgO/Cr-Ti-Si Coating System As-Coated and After 200 Hours Exposure to 2100°F (1422°K) Air.
(550X)

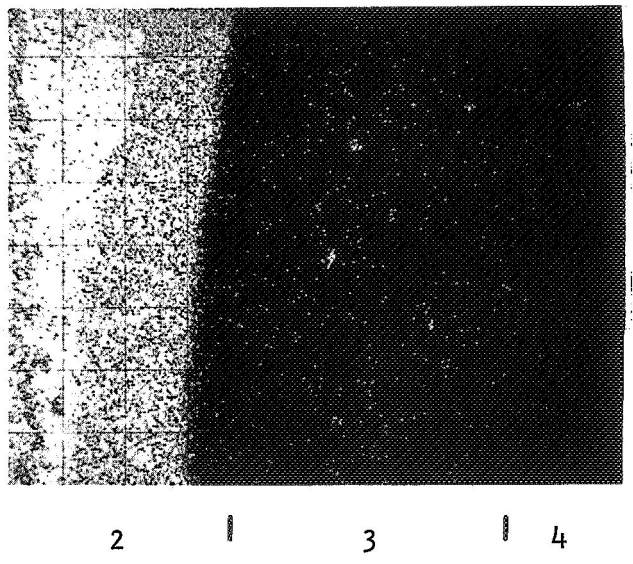

m) Si X-rays
As-Coated

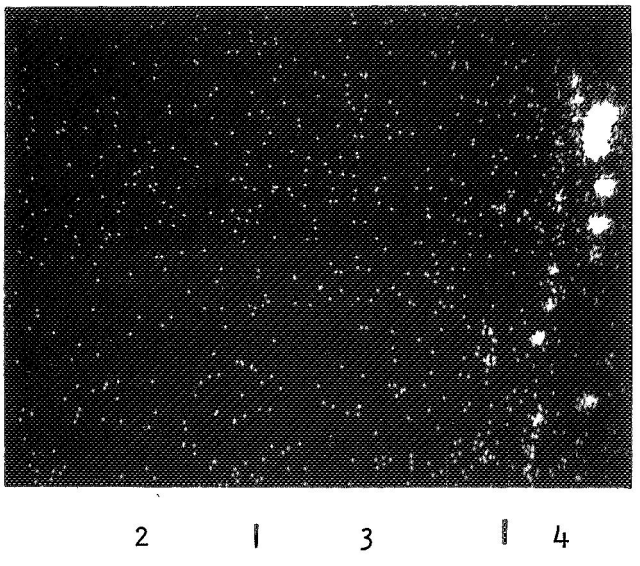

o) Y X-rays
As-Coated

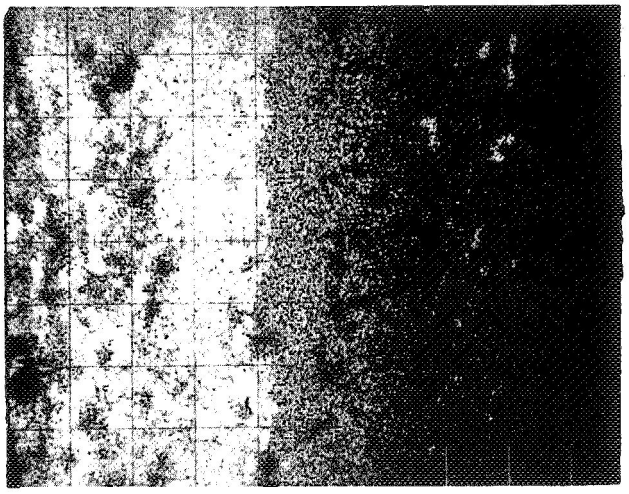

n) Si X-rays
After 200 Hours Exposure

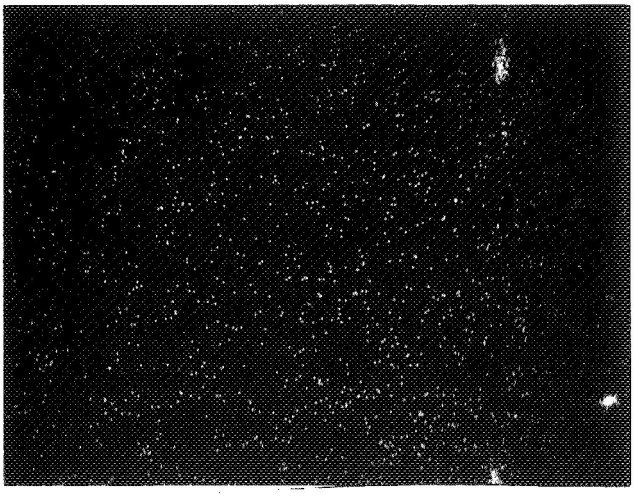

p) Y X-rays
After 200 Hours Exposure

1 Oxide
2 Coating
3 Barrier
4 Substrate

Figure 20 (Continued). Photomicrographs and EMP Images of the Cr-12MgO) Cr-Ti-Si Coating System As-Coated and After 200 Hours Exposure to 2100°F (1422°K) Air.
(550X)

370 C

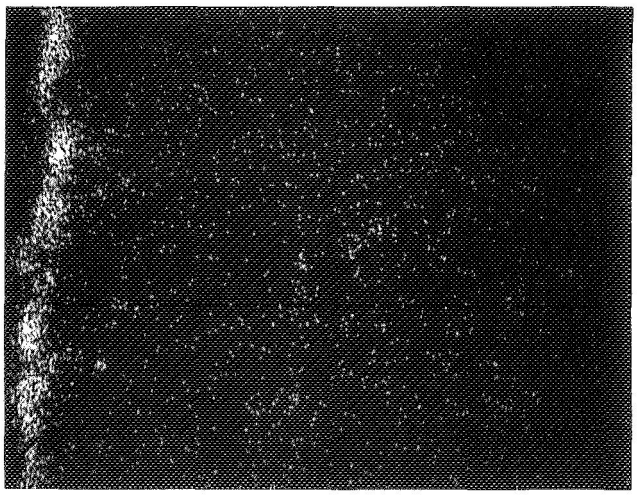

q) Al X-rays
As-Coated

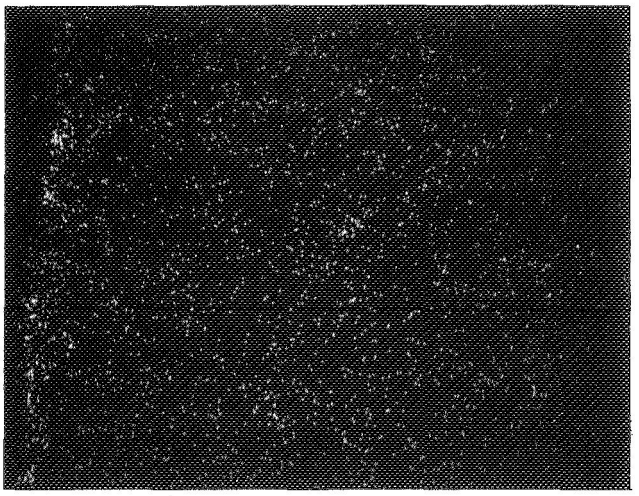

s) O X-rays
As-Coated

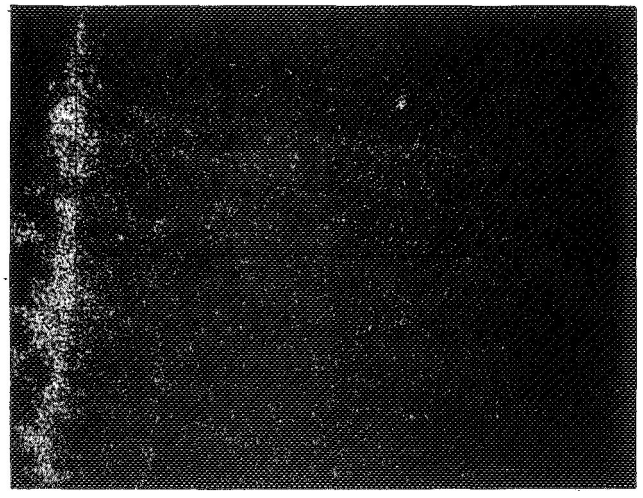

r) Al X-rays
After 200 Hours Exposure

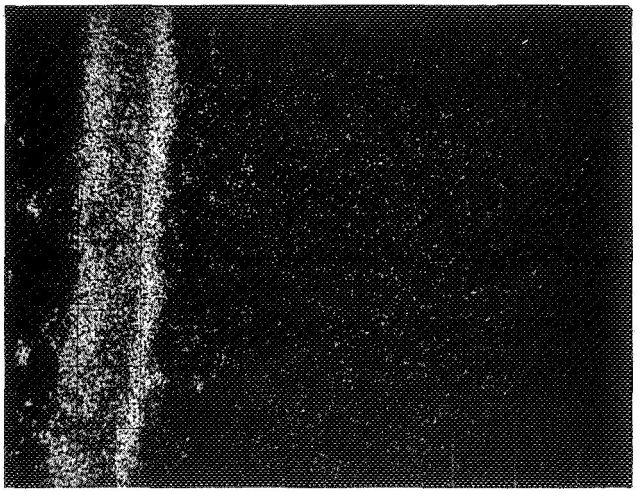

t) O X-rays
After 200 Hours Exposure

1 Oxide
2 Coating
3 Barrier
4 Substrate

Figure 20 (Continued). Photomicrographs and EMP Images of the Cr-12MgO/Cr-Ti-Si Coating System As-Coated and After 200 Hours Exposure to 2100°F (1422°K) Air.
(550X)

371 c

APPENDIX I - SUMMARY OF d° AND PEAK HEIGHTS

PEAK HEIGHT MINUS BACKGROUND FOR INDICATED SPECIMENS

d°	112-J	111-E	110-2	111-C	115-2	110-1	112-9	6	Cr-7Mo-2Ta
4.11				22					
4.07	6	10	15			9	16	30	
4.06					15				
3.63	8			27				9	
3.62		23	10		16	10	29		83
3.49	6								
3.48	21					20		20	
3.46					5				
3.39								20	
3.36							7		
3.35					6				
3.31								67	
3.30			35		18		13		
3.29		40		17	8	32			
3.25	25	32		34				40	
3.24						10			
3.23	14								
3.20					17				
3.18				10					
3.16	16	23						80	

APPENDIX I - SUMMARY OF d° AND PEAK HEIGHTS

PEAK HEIGHT MINUS BACKGROUND FOR INDICATED SPECIMENS (continued)

d°	112-J	111-E	110-2	111-C	115-2	110-1	112-9	6	Cr-7Mo-2Ta
3.15					8		12		
3.13				9					
3.12	3								
3.10		27	20	9	8	15		57	
3.09					5				
3.08							12		
2.86	4	8		4		10	22		
2.85					5				
2.73	4	8		2			14		
2.72									
2.71					3.5				
2.67			13	17				12	
2.66	6	16			9	10			
2.65							27		
2.61								10	
2.59								12	
2.58	4								
2.55	6		7	7					
2.54						18			
2.49	64		51.5	70				36	

APPENDIX I - SUMMARY OF d° AND PEAK HEIGHTS

PEAK HEIGHT MINUS BACKGROUND FOR INDICATED SPECIMENS (continued)

d°	112-J	111-E	110-2	111-C	115-2	110-1	112-9	6	Cr-7Mo-2Ta
2.48		5				61			
2.47					44		67		97
2.42	3								
2.40					3				
2.38						7			
2.36	2								
2.33								8	
2.32					5				
2.30	5			8				10	
2.29		17			6				
2.26									10
2.23	7		8						
2.22						7			
2.19	9							20	
2.18	18		19	19					
2.17		7				15	23		40
2.09	2								
2.08						20			
2.07				4					
2.06	2								

APPENDIX I - SUMMARY OF d° AND PEAK HEIGHTS

PEAK HEIGHT MINUS BACKGROUND FOR INDICATED SPECIMENS (continued)

d°	112-J	111-E	110-2	111-C	115-2	110-1	112-9	6	Cr-7Mo-2Ta
2.05		12							
2.04			6						8
1.816	5			16				8	94
1.812			11						
1.81		12					19		
1.809					7	7			
1.739	2		3			6			
1.726					9				
1.708	7								
1.705						8			
1.691				17		25		33	
1.69		12					10		
1.688	21		19						
1.674	11		15					31	
1.671				19		12			94
1.67		15					27		
1.646	12					9		20	
1.643			9						
1.628								20	
1.627	6		7						

APPENDIX I - SUMMARY OF d° AND PEAK HEIGHTS

PEAK HEIGHT MINUS BACKGROUND FOR INDICATED SPECIMENS (continued)

d°	112-J	112-E	110-2	111-C	115-2	110-1	112-9	6	Cr-7Mo-2Ta
1.625				8					
1.622					9	9			
1.601	4		6						
1.600						18			
1.579									9
1.578									
1.574									3
1.529					7				
1.483	8		8	6					
1.478						15			
1.468	6							7	
1.466			10	14		9			
1.464	11								35
1.46		12					17		
1.434	7							20	
1.432			16	26		11			51
1.43		20			16		30		
1.418						7			
1.403						6			
1.38							6		

APPENDIX I - SUMMARY OF d° AND PEAK HEIGHTS

PEAK HEIGHT MINUS BACKGROUND FOR INDICATED SPECIMENS (continued)

d°	112-J	111-E	110-2	111-C	115-2	110-1	112-9	6	Cr-7Mo-2Ta
1.379			6						
1.374						11			
1.370	8		10						
1.363								12	
1.360									
1.355			6						
1.353	4					7			
1.338	2								
1.336			5						
1.297									17
1.247	2								
1.240	3	3	4	6			7		9
1.237					4				
1.210									5

DISTRIBUTION LIST

NASA Headquarters
600 Independence Avenue
Washington, D. C. 20546
Attn: RAP/N.F.Rekos

NASA Headquarters
600 Independence Avenue
Washington, D. C. 20546
Attn: RRM/G. C. Deutch

NASA Headquarters
600 Independence Avenue
Washington, D. C. 20546
Attn: RRM/R. H. Raring

NASA-Ames Research Center
Moffett Field, California 94035
Attn: Library

NASA-Flight Research Center
P. O. Box 273
Edwards, California 93523
Attn: Library

NASA-Goddard Space Flight Center
Greenbelt, Maryland 20771
Attn: Library

Jet Propulsion Laboratory
4800 Oak Grove Drive
Pasadena, California 91102
Attn: Library

NASA-Langley Field, Virginia 23365
Attn: 214/Irvin Miller

NASA-Langley Research Center
Langley Field, Virginia 23365
Attn: Library

NASA-Manned Space Flight Center
Houston, Texas 77058
Attn: Library

NASA-Marshall Space Flight Center
Huntsville, Alabama 35812
Attn: Library

Air Force Office of Scientific Research
Propulsion Research Division
USAF Washington, D. C. 20525
Attn: Library

Defense Documentation Center (DDC)
Cameron Station
5010 Duke Street
Alexandria, Virginia 22314

NASA-Lewis Research Center
21000 Brookpark Road
Cleveland, Ohio 44135
Attn: 105-1/G. M. Ault

NASA-Lewis Research Center
21000 Brookpark Road
Cleveland, Ohio 44135
Attn: 3-19/Technology Utilization Office

NASA-Lewis Research Center
21000 Brookpark Road
Cleveland, Ohio 44135
Attn: 49-1/S. Grisaffe

NASA-Lewis Research Center
21000 Brookpark Road
Cleveland, Ohio 44135
Attn: 105-1/N. T. Saunders

NASA-Lewis Research Center
21000 Brookpark Road
Cleveland, Ohio 44135
Attn: Library (60-3) (3)

NASA-Lewis Research Center
21000 Brookpark Road
Cleveland, Ohio 44135
Attn: 5-5/Report Control Office

NASA-Lewis Research Center
21000 Brookpark Road
Cleveland, Ohio 44135
Attn: 106-1/R. E. Oldrieve

DISTRIBUTION LIST
(Continued)

NASA-Lewis Research Center
21000 Brookpark Road
Cleveland, Ohio 44135
Attn: 105-1/J. R. Stephens (2)

NASA-Lewis Research Center
21000 Brookpark Road
Cleveland, Ohio 44135
Attn: 49-1/J. P. Merutka (15)

NASA-Lewis Research Center
21000 Brookpark Road
Cleveland, Ohio 44135
Attn: 77-3/L. W. Schopen

NASA-Lewis Research Center
21000 Brookpark Road
Cleveland, Ohio 44135
Attn: 105-1/W. D. Klopp (2)

NASA-Lewis Research Center
21000 Brookpark Road
Cleveland, Ohio 44135
Attn: 105-1/R. W. Hall

NASA-Lewis Research Center
21000 Brookpark Road
Cleveland, Ohio 44135
Attn: 49-1/J. C. Freche

NASA-Lewis Research Center
21000 Brookpark Road
Cleveland, Ohio 44135
Attn: 49-1/H. B. Probst

NASA Scientific & Tech. Information
P. O. Bx 33 Fac.
College Park, Maryland 20740 (6)

FAA Headquarters
800 Independence Avenue, S. W.
Washington, D. C. 20553
Attn: Brig. Gen. J. C. Maxwell

FAA Headquarters
800 Independence Avenue, S. W.
Washington, D. C. 20553
Attn: SS/210/F. B. Howard

U. S. Atomic Energy Commission
Washington, D. C. 20545
Attn: Technical Reports Library

Oak Ridge National Laboratory
Oak Ridge, Tennessee 37830
Attn: Technical Reports Library

Department of the Navy
ONR
Code 429
Washington, D. C. 20525

Headquarters
Wright-Patterson AFB, Ohio 45433
Attn: MAMP

Headquarters
Wright-Patterson AFB, Ohio 45433
Attn: MATB

Headquarters
Wright-Patterson AFB, Ohio 45433
Attn: MAAM/Technical Library

Headquarters -Attn: AFSC-FTDS
Wright-Patterson AFB, Ohio 45433

Headquarters
Wright-Patterson AFB, Ohio 45433
Attn: AFML:MAM

Headquarters
Wright-Patterson AFB, Ohio 45433
Attn: MAG/Directorate of Materials

U. S. Army Aviation Materials Laboratory
Port Eustis, Virginia 23604
Attn: SMOFE-APG/John White, Chief

Bureau of Naval Weapons
Department of the Navy
Washington, D. C. 20525
Attn: RRMA-2/T. F. Kearns, Chief

Army Materials Research Agency
Watertown Arsenal
Watertown, Massachusetts 02172
Attn: Director

DISTRIBUTION LIST
(Continued)

Battelle Memorial Institute
505 King Avenue
Columbus, Ohio 43201
Attn: Defense Metals Information
Center (DMIC)

Battelle Memorial Institute
505 King Avenue
Columbus, Ohio 43201
Attn:Dr. R. I. Jaffe

Aerospace Corporation
Reports Acquisition
P. O. Box 95085
Los Angeles, California 90045

Advanced Metals Research Corporation
149 Middlesex Turnpike
Burlington, Massachusetts 01804
Attn: J. T. Norton

Allegheny Ludlum Steel Corporation
Research Center
Alabama and Pacific Avenues
Prackenridge, Pennsylvania 15014
Attn: Library

American Society for Metals
Metals Park
Novelty, Ohio 44073
Attn: Library

Avco Space Systems Division
Lowell Industrial Park
Lowell, Massachusetts 01851
Attn: Library

The Bendix Corporation
Research Laboratories Division
Southfield, Michigan 48075
Attn: Library

Boeing Company
P. O. Box 733
Renton, Washinton 98055
Attn: SST Unit Chief, W. E. Binz

Case Institute of Technology
University Circle
Cleveland, Ohio 44106
Attn: Library

Chromalloy Corporation
169 Western Highway
West Nyack, New York 10994
Attn: Mr. L. Maisel

Denver Research Institute
University Park
Denver, Colorado 80210
Attn: Library

Douglas Aircraft Company MFSD
3000 Ocean Park Boulevard
Santa Monica, California 90406
Attn: Library

Fansteel Metallurgical Corporation
Number One Tantalum Place
North Chicago, Illinois 60064
Attn: Library

Ford Motor Company
Materials Development Dept.
20000 Rotunda Drive
P. O. Box 2053
Dearborn, Michigan 48123
Attn: Mr. Y. P. Telang

Firth Sterling, Inc.
Powder Metals Research
P. O. Box 71
Pittsburgh, Pennsylvania 15230
Attn: Library

General Electric Company
Advanced Technology Laboratory
Schenectady, New York 12305
Attn: Library

General Electric Company
Materials Development Lab. Oper.
Advance Engine and Tech. Dept.
Cincinnati, Ohio 45215
Attn: Mr. L. P. Jahnke

DISTRIBUTION LIST
(Continued)

General Motors Corporation
Allison Division
Indianapolis, Indiana 46206
Attn: Mr. D. K. Hanink,
Materials Laboratory

General Technologies Corporation
708 North West Street
Alexandria, Virginia 22314
Attn: Library

E. I. DuPont de Nemours and Co.,Inc.
Pigments Dept. Metal Products
Wilmington, Delaware 19898
Attn: Library

IIT Research Institute
Technology Center
Chicago, Illinois 60616
Attn: Mr. V. Hill

IIT Research Institute
Technology Center
Chicago, Illinois 60616
Attn: Library

Ilikon Corporation
Natick Industrial Center
Natick, Massachusetts
Attn: Library

International Nickel Company
P. D. Merica Research Laboratory
Sterling Forest
Suffern, New York 10901
Attn: Library

Arthur D. Little, Inc.
20 Acorn Park
Cambridge, Massachusetts
Attn: Library

Lockheed Palo Alto Research Labs.
Materials and Science Lab. 52-30
3251 Hanover Street
Palo Alto, California 94304
Attn: Roger Perkins

Lockheed Palo Alto Research Labs.
Materials and Science Lab. 52-30
3251 Hanover Street
Palo Alto, California 94304
Attn: Mr. E. C. Burke

Massachusetts Institute of Technology
Metallurgy Dept., RM-8-305
Cambridge, Massachusetts 02139
Attn: Library

Narmco Research & Development Div.
Whittaker Corporation
3540 Aero Court
San Diego, California 92123
Attn: Library

AFML (MAMP)
Wright-Patterson AFB, Ohio 45433
Attn: Mr. N. Geyer

Bureau of Naval Weapons
Department of the Navy
Washington, D. C. 20525
Attn: Mr. I. Machlin

Alloy Surfaces, Inc.
100 South Justison Street
Wilmington, Delaware 19899
Attn:Mr. George H. Cook

Battelle Memorial Institute
505 King Avenue
Columbus, Ohio 43201
Attn: Mr. E. Bartlett

City College of New York
Department of Chemical Engineering
New York, New York 10031
Attn: Mr. R. A. Graff

City College of New York
Department of Chemical Engineering
New York, New York 10031
Attn: Mr. M. Kolodney

DISTRIBUTION LIST
(Continued)

E. I. DuPont de Nemours and Company
1007 Market Street
Wilmington, Delaware 19898
Attn: Dr. Warren I. Pollack

General Electric Company
Materials Development Lab. Oper.
Advance Engine and Tech. Dept.
Cincinnati, Ohio 45215
Attn: Mr. M. Levinstein

General Electric Company
Materials Development Lab. Oper.
Advance Engine and Tech. Dept.
Cincinnati, Ohio 45215
Attn: Mr. J. W. Clark

Howmet Corporation
Misco Division
One Misco Drive
Whitehall, Michigan 49461
Attn: Mr. S. Wolosin

Pratt & Whitney
Division of United Aircraft Corp.
Manufacture Engineering
Aircraft Road
Middletown, Connecticut 06457
Attn: Mr. Frank Talboom

Sylvania Electric Products
Sylcor Division
Cantiague Road
Hicksville L.I., New York 11802
Attn: Mr. L. Sama

Texas Instruments, Inc.
Materials and Controls Division
P. O. Box 5474
Dallas, Texas 75222
Attn: Mr. Gene Wakefield

U.S.A.F.
San Antonio Air Material Area
Kelley Air Force Base, Texas 78241
Attn: SANEPJ/A. E. Wright, Chief
Jet Engine Section

University of Dayton
Research Institute
300 College Park Avenue
Dayton, Ohio 45409
Attn: Library

University of Illinois
Department of Ceramic Engineering
Urbana, Illinois 61801
Attn: Mr. J. Wurst

Nuclear Materials Company
West Concord, Massachusetts 01781
Attn: Library

Ohio State University
Columbus, Ohio 43210
Attn: Library

Rensselaer Polytechnic Institute
Troy, New York 12180
Attn: Library

Sherritt Gordon Mines, Ltd.
Research and Development Div.
Fort Saskatchewan, Alberta, Canada
Attn: Library

Spartan Aviation, Inc.
Aviation Services Division
P. O. Box 51239
Dawson Station
Tulsa, Oklahoma 07052
Attn: Mr. M. Ortner

Stanford Research Institute
Menlo Park, California
Attn: Library (Technical)

Stanford University
Palo Alto, California 94305
Attn: Library

Union Carbide Corporation
Stellite Division
Technology Department
Kokomo, Indiana 46901
Attn: Library (Technical)

DISTRIBUTION LIST
(Continued)

United Aircraft Corporation
400 Main Street
East Hartford, Connecticut 06108
Attn: Research Library

United Aircraft Corporation
400 Main Street
East Hartford, Connecticut 06108
Attn: E. F. Bradley, Chief
Materials Engineering

United Aircraft Corporation
Pratt and Whitney Division
West Palm Beach, Florida 33402
Attn: Library

Universal-Cyclops Steel Corporation
Bridgeville, Pennsylvania 15017
Attn: Library

Wah Chang Corporation
Albany, Oregon 97321
Attn: Library

Westinghouse Electric Corporation
Westinghouse Astronuclear Lab.
P. O. Box 10864
Pittsburgh, Pennsylvania 15236
Attn: Mr. W. Buckman

University of Pittsburgh
Center for Study of Thermodynamic
Properties of Materials
409 Engineering Hall
Pittsburgh, Pennsylvania 15213
Attn: Dr. G. R. Fitterer

University of Washington
Ceramics Department
Seattle,Washington 98101
Attn: Dr. J. Mueller

Westinghouse Electric Corporation
Research Laboratories
Beulah Road, Churchill Buro.
Pittsburgh, Pennsylvania 15235
Attn: Mr. R. Grekila

Whitfield Laboratories
P. O. Box 287
Bethel, Connecticut 06801